Role of an N2-Src-COPII pathway in neuroblastoma differentiation

Elisa Redavide

MSc by Research

University of York

Biology

September 2017

Abstract

Neuroblastoma is the most common extracranial solid tumour in childhood and nearly half of neuroblastoma cases occur in children less than two years of age. This cancer is thought to arise due to an alteration during neuronal differentiation and only 30 % of patients with high-risk tumours survive. High-risk neuroblastoma cases are treated with retinoic acid to induce differentiation of the tumour cells left after tumour resection, but these tumours are usually refractive to retinoic acid and other post-surgery therapies. Intriguingly, a positive outcome for low risk disease correlates with high expression levels in the tumour of a neuronal isoform of the ubiquitously expressed C-Src kinase, N2-Src kinase, which is thought to induce spontaneous differentiation of the neuroblastoma to a harmless neuronal phenotype. Indeed, preliminary experiments in our laboratory have shown that overexpression of N2-Src in retinoic acid-resistant neuroblastoma cells is sufficient to differentiate them. It was also shown that N2-Src kinase interacts with proteins of the COPII complex, which coats secretory vesicles that traffic from the ER to the Golgi apparatus, and, interestingly, a preliminary finding showed that the overexpression of the COPII protein Sec23A disrupts N2-Src-dependent differentiation.

In this study, I investigated the interplay between N2-Src and the COPII complex in an inducible N2-Src expressing cell line. The aims of my research were to i) understand how N2-Src regulates COPII transport and to ii) design and validate a tool that can be used to understand whether the N2-Src dependent effects on cell morphology and migration require the COPII complex. I observed the trend of N2-Src decreasing migration, both in a random migration assay and in a wound healing assay. Moreover, an assay for COPII transport revealed a trend of N2-Src increasing the number of secretory vesicles. Furthermore, these vesicles were eventually redistributed along neurite-like processes that the cells extend when they express the kinase. I also designed and validated some shRNA constructs able to silence the protein expression of the COPII coat protein Sec23A, which could be used to verify if the silencing of this protein increases N2-Src-dependent differentiation.

Taken together, these data lead to the conclusion that N2-Src might regulate COPII transport. Future differentiation therapies for neuroblastoma could be targeted to the N2-Src/COPII pathway.

Table of Contents

List of figures

List of tables

Acknowledgements

I would like to thank Gareth Evans for his excellent supervision, council and encouragement during my project. I also appreciated a lot the help I received from the Laura West, who have provided a friendly and supportive lab environment over the year and whose company I have very much enjoyed.

Author’s declaration

I declare that this thesis is my own original work and that all external sources of information have been appropriately acknowledged. This work has not previously been submitted for any award.

1. Introduction

1.1. An overview of neural development

Mammalian neural development is one of the earliest processes to begin and the last to be completed after birth. This process generates the most complex structure within the embryo and the long period of development means *in utero* insult during pregnancy may have consequences for the development of the nervous system.

Neurulation is the folding process in vertebrate embryos through which the neural plate is transformed into the neural tube (Larsen 2001). After the formation of the neural plate (Fig. 1A), the edges of this structure thicken and move upward to form the neural fold. This generates the neural groove, which starts to divide the future right and left sides of the embryo (Fig. 1B). Eventually, the migrating neural fold fuses to form the neural tube beneath the overlaying ectoderm and the cells at the most dorsal portion of this structure become the neural crest cells (Fig. 1C) (Darnell and Gilbert 2017, Nikolopoulou et al. 2017).

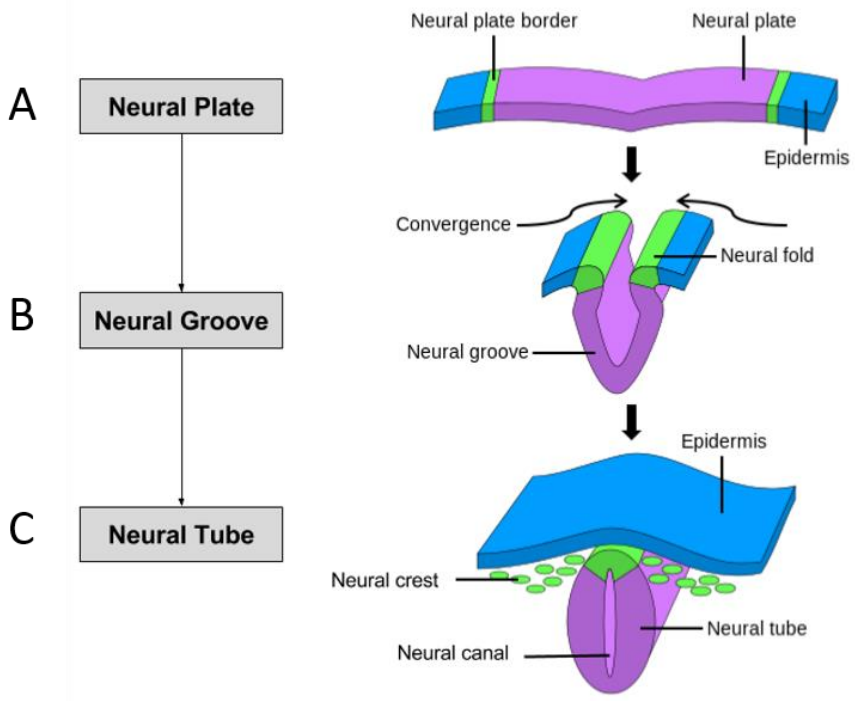

Figure 1. Overview of neurulation. Schematic representation of neurulation, which involves the elevation of the neural folds from the neural plate (A), their bedding to form the neural groove (B) and eventually fusion to form the neural tube (C) (adapted from Binz (2016)).

The neural crest structure can be divided into four domains that will generate different cell types (Bronner and LeDouarin 2012): the cephalic neural portion, which will produce the craniofacial mesenchyme that differentiate into the skeletal and connective tissue components of the head; the trunk neural crest, whose cells will become melanocytes and sensory neurons of the dorsal root ganglia; the vagal and sacral portion, which will generate the enteric ganglia of the gut; the cardiac neural crest, which can develop into melanocytes, neurons, cartilage, and connective tissue, but will also produce the musculo-connective tissue wall of the large arteries, as well as the septum that separates the pulmonary circulation from the aorta (Le Lièvre and Le Douarin 1975).

The neuroblast progenitors that will generate the sympathetic ganglia originate from neural crest progenitors in the trunk region of the embryo and follow a ventral migratory pathway from the neural crest and around the neural tube, to a region that is lateral to the notochord and dorsal aorta (Marshall et al. 2014). In this area, they receive signals from the somites, the ventral part of the neural tube, the notochord and the dorsal aorta (Huber 2006).

An important transcription factor that is normally expressed during the sympathoadrenal development is the MYCN proto-oncogene. MYCN belongs to the MYC proto-oncogene family, which includes two other paralogous proto-oncogenes (c-MYC and MYCL) that are all located on different chromosomes and expressed at specific times during development (Mathsyaraja and Eisenman 2016, Wilde and Ayer 2015). MYCN is situated on the human chromosome 2p24.3 (Schwab et al. 1984) and is a transcription factor that belongs to a class of proteins that contain a basic-region/helix-loop-helix/leucine-zipper (bHLHZip), important for protein dimerization and sequence-specific DNA binding (Gherardi et al. 2013). This proto-oncogene is important in regulating processes such as cell growth, differentiation and apoptosis, but aberrant regulation of MYCN is often observed in cancers and can lead to dysregulated cell proliferation (Wilde and Ayer 2015).

During normal sympathoadrenal development, MYCN expression is high in the post migratory neural crest cells because it regulates the migration and expansion of the neural crest cells (Zimmerman et al. 1986). Its levels are subsequently reduced when the cells are differentiating into sympathetic neurons. While the excess neural precursors undergo apoptotic cell death, a process promoted by neural growth factor (NGF) deprivation (Yuan and Yankner 2000), the bone morphogenetic protein (BMP) signalling derived from the dorsal aorta promotes the specification of the neuronal and catecholaminergic properties of the

primary sympathetic ganglia (Huber 2006, Reissmann et al. 1996, Schneider et al. 1999). It is believed that the aberrant differentiation of neural crest cells during development causes the tumour pathology associated with childhood neuroblastoma (Marshall et al. 2014).

1.2. Neuroblastoma

The onset of cancer is a multi-step process that induces genomic instability and life-threatening cellular phenotypes. However, the evidence that a minority of cancer cells possess embryonal features or the plasticity to revert to embryonal features during postnatal life has led to the cancer stem cell hypothesis (Valent et al. 2012), which describes the heterogeneity that is evident in tumours.

In some childhood cancers such as neuroblastoma, the precursor hyperplasia of embryonal cells has a tendency to undergo spontaneous regression and cell death (Nuchtern et al. 2012). It is known that during embryogenesis many more cells are produced than are required for organogenesis but mechanisms such as trophic factor withdrawal remove cells that are in excess after organogenesis is complete. Unfortunately, in some cases embryonal cells can resist cell death signals, and later acquire additional alterations, which can lead to postnatal malignant transformation (Marshall et al. 2014).

Neuroblastoma is the most common extracranial solid tumour in childhood and nearly half of neuroblastoma cases occur in children less than two years of age (Stafman and Beierle 2016). Neuroblastoma arises from the sympathoadrenal lineage of the neural crest, and therefore tumours can develop anywhere in the sympathetic nervous system (Maris et al. 2007). There have been several staging systems for neuroblastoma, but currently the most widely used is the International Neuroblastoma Staging System (INSS), which combines clinical and surgical staging (Brodeur et al. 1993, Goldsby and Matthay 2004, Matthay et al. 2016). This system comprises 5 different stages of neuroblastoma, relating to risk: the low-risk group is composed of patients with Stage 1, 2A and 2B neuroblastoma, who all have localized tumours with or without complete gross excision; the intermediate group comprises Stage 3 patients, who have an unresectable unilateral tumour; and finally the high-risk group, which includes Stage 3 patients with an unresectable tumour *and* MYCN amplification, and Stage 4 patients, who have a primary tumour with dissemination to distant lymph nodes, bone marrow, liver and other organs (Brodeur et al. 1993). The INSS also identifies Stage 4S,

which represents a specific subset of patients younger than 1 year old, with tumours that tend to spontaneously remit (Goldsby and Matthay 2004).

Many clinical and experimental features link neuroblastoma to altered embryogenesis (Marshall et al. 2014). A significant percentage of stage 4S patients with neuroblastoma in early childhood have spontaneous regression without therapy. Moreover, the autopsies of sympathoadrenal tissues from children whose cause of death was not cancer show an incidence of neuroblast pre-cancer cells that is higher than the incidence of clinical neuroblastoma (Beckwith and Perrin 1963). Patients' biopsies show that the tumour cells are arrested at various stages of neuronal differentiation and the grade of differentiation correlates with clinical course (Wilson and Draper 1974). It seems likely that neuroblastoma cells develop due to an alteration in neural differentiation, because the majority of neuroblastomas continue to express the MYCN proto-oncogene (Matsunaga et al. 1993). Furthermore, the more aggressive high risk tumours have MYCN gene amplification (Brodeur et al. 1993).

Another factor that seems to have a role in the dysregulation of neural differentiation is the anaplastic lymphoma receptor tyrosine kinase (ALK) (Chen et al. 2008, George et al. 2008, Janoueix-Lerosey et al. 2008, Mosse et al. 2008). It seems that ALK plays a role in the normal development of the central and peripheral nervous system since it localizes primarily to spinal motor neurons, the sympathetic ganglia, and the dorsal root ganglia during development (Degoutin et al. 2009, Hurley et al. 2006, Iwahara et al. 1997, Morris et al. 1997, Vernersson et al. 2006), where it is thought to regulate the balance between proliferation and differentiation (Cheng and Ott 2010, Mosse, Wood, and Maris 2009, Palmer et al. 2009).

MYCN amplification, along with ALK mutations or amplification, could give resistance to trophic factor withdrawal signals during neuroblastoma initiation, since MYCN acts as a classical transcription factor, promoting migration and the expression of individual genes that increase cell proliferation (Stafman and Beierle 2016). One of the factors regulated by MYCN is the C-Src proto-oncogene, which encodes a membrane-bound tyrosine specific protein kinase. In a previous study of human neuroblastoma by Mellstrom et al. (1987) C-Src expression was found to correlate positively with neuronal/neuroendocrine differentiation, as measured by neuron-specific enolase expression. In addition, later studies by Bjelfman et al. (1990), Hedborg et al. (1995) and Matsunaga et al. (1993, 1998) found that the high expression of N2-Src, a neuronal isoform of C-Src, was indicative of a higher degree of

differentiation or differentiation potential, making this gene a useful biomarker for prognostic evaluation of infant neuroblastoma.

1.3. Neuroblastoma therapies

Since clinical heterogeneity is a hallmark of neuroblastoma, current treatments involve a risk-based approach based on combinations of clinical and biological prognostic markers (Cohn et al. 2009). For patients with low- or intermediate-risk neuroblastoma, who have excellent outcomes, surgery alone (De Bernardi et al. 2008) or a reduced treatment of chemotherapy and resection of the tumour (Rubie et al. 2011) are curative. However, patients with high-risk tumours with MYCN amplification undergo cycles of chemotherapy, plus surgery and radiotherapy for residual local and metastatic disease (Matthay et al. 1999, Matthay et al. 2009). These approaches have resulted in improved outcomes, although survival for high-risk patients remains poor, emphasizing the need for more effective treatments (Pinto et al. 2015).

One of the therapies used as a maintenance treatment with high-risk neuroblastoma patients is 13-cis-retinoic acid (Matthay et al. 2009, Matthay et al. 1999). Endogenous retinoic acid signalling regulates proliferation, differentiation, and inflammation, although the exact mechanisms of action are still unknown (Bushue and Wan 2010). Retinoic acid (RA) derives from vitamin A and is a small lipophilic molecule that binds nuclear RA receptors (RARs) (Kleiner-Bossaler and Deluca 1971). The binding of RA to a RAR causes the formation of a heterodimer complex between RAR and retinoid X receptor (RXR). The RAR–RXR complex modulates transcription by binding to DNA at RA response elements (RAREs) located in enhancer regions of RA target genes (Duester 2008, Niederreither and Dolle 2008). Endogenous RA has an important role during normal development, since it has been seen to contribute to the anteroposterior patterning of the neural plate (Glover, Renaud, and Rijli 2006), to the development of the spinal cord and somites (Diez del Corral et al. 2003). In addition, it makes a fundamental contribution to the development of organs and limbs (Cunningham and Duester 2015) and the differentiation of the neural retina at later stages of development (Kelley, Turner, and Reh 1994).

Exogenous RA is used by researchers to study the differentiation of neuroblastoma cell lines, such as SH-SY5Y cells (Acosta et al. 2009). Nevertheless, some cell lines like SK-N-LP or LA1-55N do not show changes in morphology when treated with this molecule (Acosta et

al. 2009). Moreover, exogenous RA is usually only effective against minimal residual disease and does not prevent recurrence from larger tumours, thus leading researchers to seek new differentiation strategies for refractory tumours.

A poorly characterised neuronal splice variant of the C-Src protein, N2-Src, was previously shown to correlate with neuronal differentiation and neuroblastoma outcome for patients (Mellstrom et al. 1987, Bjelfman et al. 1990, Matsunaga et al. 1993, Hedborg et al. 1995, Matsunaga et al. 1998), therefore being a potential novel differentiation factor that will be investigated in this study.

1.4. Src kinase

The Src family of non-receptor tyrosine kinases (SFKs) plays a fundamental role in multiple cellular processes, including proliferation, differentiation, migration and membrane trafficking (Roskoski 2015).

The SFK family shares a conserved structure (Fig. 2), which contains from the N- to C-terminus (Brown and Cooper 1996, Thomas and Brugge 1997): an N-terminal 14-carbon myristoyl group SH4 domain, which facilitates the attachment of Src to membranes and is required for Src's function in cells (Brown and Cooper 1996); a unique domain, exclusive to all members of the SFK family; an SH3 domain and an SH2 domain, which participate in substrate interaction; an SH1 protein-tyrosine kinase domain (catalytic domain), that provides the kinase activity and possesses an autophosphorylation site (Tyr 416) that promotes the catalytic activity (Brown and Cooper 1996); a C-terminal regulatory segment, which contains a tyrosine residue (Tyr 527) that, if phosphorylated, negatively regulates the kinase activity (Brown and Cooper 1996) (Fig. 2).

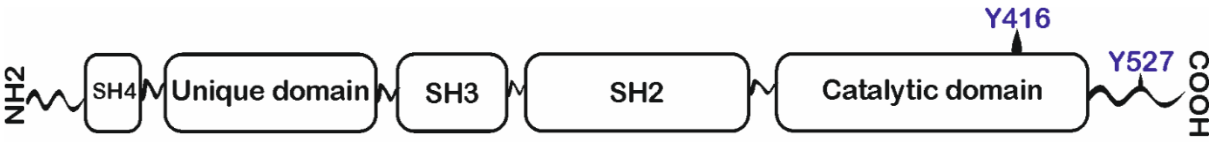

Figure 2. Organization of Src. The ~60 kDa Src protein comprises a myristoylated SH4 domain, a unique domain, an SH3 domain, an SH2 domain, the catalytic domain (SH1) and a C-terminal tail.

Regulation of Src activity relies to a large extent on two intramolecular interactions (Xu et al. 1999, Roskoski 2015). Firstly, phosphorylation of Tyr 527 in the C-terminal tail promotes binding to the SH2 domain, thus favouring an inactive conformation (Fig. 3). Secondly, the SH3 domain binds to a proline-rich motif in the linker between the SH2 and the

kinase catalytic domain (Fig. 3). Different mechanisms of activation have been reported for each member of the SFK family and these include (Moroco et al. 2014): displacement of the SH3 domain from the SH2-kinase linker (Briggs and Smithgall 1999), displacement of the C-terminal tail from the SH2 domain (Brown and Cooper 1996), displacement of both these intramolecular interactions (Thomas et al. 1998), and trans-phosphorylation of the activation loop tyrosine by a different kinase (Chong et al. 2004). Indeed, displacement of the intramolecular regulatory interactions involving the SH2 and the SH3 domains can determine kinase activation, promoting a change in the linker conformation and the autophosphorylation of the Tyr 416. In particular, it has been shown that C-Src seems more susceptible to activation after the SH3 domain displacement (Moroco et al. 2014). Therefore, not only the displacement of the SH2 or SH3 domains by the binding to phosphotyrosine or Pro-X-X-Pro motifs respectively in target proteins, but also the dephosphorylation of Tyr 527 determines the activation of the kinase (Sicheri and Kuriyan 1997, Sicheri, Moarefi, and Kuriyan 1997). These events induce disassembly of the intramolecular interactions and, in addition, Tyr 416 in the kinase domain is exposed for subsequent autophosphorylation to elicit full kinase activity (Fig. 3).

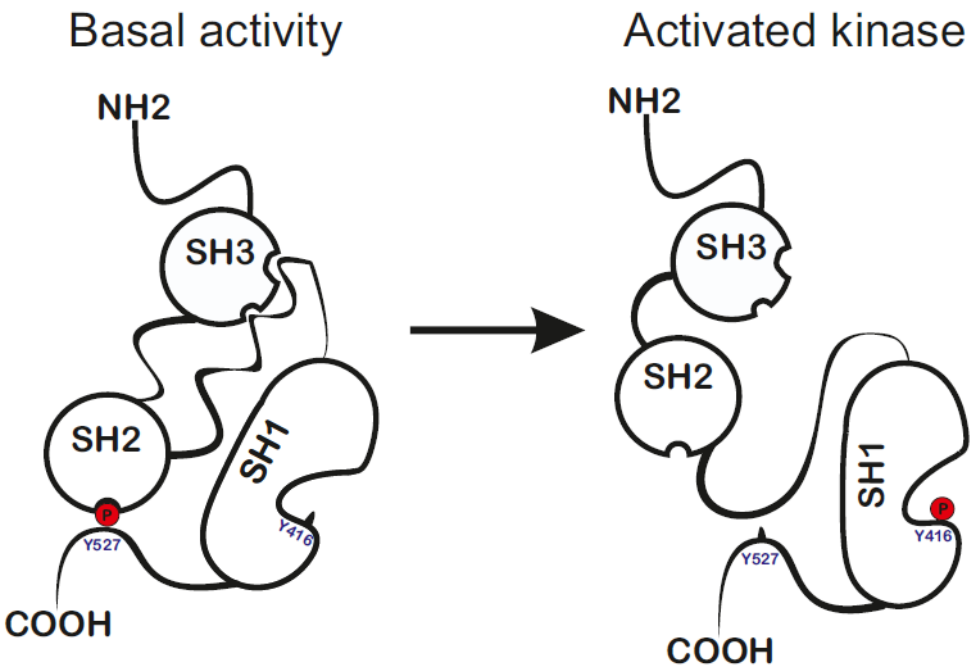

Figure 3. Regulation of Src activity. The regulation of Src kinase relies on the phosphorylation of Tyr 527 in the C-terminal: when this tyrosine is phosphorylated, it binds to the SH2 domain, promoting an inactive conformation. Dephosphorylation of Tyr 527 or binding of ligands to the SH2 or SH3 domains favour intramolecular interactions which expose Tyr 416 for autophosphorylation that enables full kinase activity.

1.4.1. C-Src kinase

C-Src is one of eleven members of the SFKs, ubiquitously expressed in vertebrate cells (Hoffmann et al. 1983, Parker et al. 1985), and it is involved in the regulation of multiple processes, from cell growth, differentiation and cell shape, to migration and survival (Parsons and Parsons 2004).

A homologue of C-Src, v-Src, was first found in 1910 by Peyton Rous while he was studying the Rous sarcoma virus (RSV), a chicken retrovirus. V-Src is an activated form of C-Src kinase that is capable of causing tumours in chickens and transforming cells in culture with high efficiency (Rous 1910b, a) and is encoded by the first oncogene to be discovered (Martin 2001). It was many years later when the cellular form of v-Src kinase, pp60c-src or C-Src, was discovered in uninfected cells (Oppermann et al. 1979, Collett et al. 1979). The subsequent molecular cloning and sequencing of the chicken C-Src gene and the RSV v-Src gene showed that the cellular C-Src oncogene and the RSV v-Src are closely related (Hanafusa 1987, Parker, Varmus, and Bishop 1981, Shalloway, Zelenetz, and Cooper 1981, Takeya, Feldman, and Hanafusa 1982). However, these genes differ at their C-terminal regulatory segment: 19

amino acids of the chicken C-Src are replaced by 12 completely different amino acids in the RSV v-Src, thus interfering with its regulation and therefore activity (Takeya and Hanafusa 1983). Eventually, it was found that there are other viral strains, which contain mutations in other domains of the protein (Martin 2004).

In cells, C-Src is usually maintained in an inactive state through phosphorylation of Tyr 527 in the C-terminal regulatory domain (Fig. 3), but it can be activated during cellular events such as mitosis, or in abnormal events such as by mutation in some human cancers (Bjorge, Jakymiw, and Fujita 2000, Ishizawar and Parsons 2004).

In the nervous system, C-Src kinase is widely expressed and abundant in neuronal cells, where it is involved in proliferation and differentiation during development of the central nervous system, but it is also highly expressed in fully differentiated neurons, suggesting that it regulates additional processes (Parsons and Parsons 2004). Many studies show that Src's function is to upregulate the activity of N-methyl-D-aspartate (NMDA) receptors and other ion channels and receptors (Kalia, Gingrich, and Salter 2004), thus controlling processes underlying physiological plasticity, such as learning and memory, but also in disease, for example in pain and epilepsy (Parsons and Parsons 2004). C-Src is enriched in presynaptic nerve terminals, where it has been shown to interact with synapsin I and synaptophysin (Onofri et al. 2007). Synapsin I is an abundant synaptic vesicles (SV)-associated phosphoprotein, which has a pivotal role in mature neurons in regulating neurotransmitter release and short term synaptic plasticity, but also during development where it regulates synaptic connectivity (Baldelli et al. 2007, Hilfiker et al. 1999). It has been shown that the proline-rich COOH-terminal of synapsin I interacts with the SH3 domain of C-Src (McPherson et al. 1994, Onofri et al. 2000), thus stimulating its tyrosine kinase activity, which could be physiologically relevant for the neuronal signal transduction pathways mentioned above (Onofri et al. 1997, Onofri et al. 2007). Synaptophysin is the most abundant tyrosine phosphorylated protein in the synapse, but its function is still not clear (Evans and Cousin 2005). Clues have come from experiments demonstrating that C-Src activates TI-VAMP exocytosis *in vitro* by phosphorylating its Longin domain (Burgo et al. 2013). In particular, it has been seen that the interaction between C-Src and synaptophysin is increased *in vivo* during learning tasks, where long term potentiation (LTP) was proven to increase tyrosine phosphorylation on synaptophysin (Mullany and Lynch 1998, Zhao et al. 2000).

C-Src has two splice variants expressed solely in neuronal tissue (Brugge et al. 1985, Pyper and Bolen 1989), termed N1- and N2-Src (Fig. 4). The N-Srcs' additional amino acids are inserted in the so-called 'n-src' loop of the SH3 domain, changing its interaction interface and dramatically affecting its binding specificity (Keenan et al. 2015). N1-Src arises from an insertion of the N1 mini-exon (six amino acids), while in N2-Src the N1 and N2 mini exons insert a total of seventeen amino acids (Fig. 4).

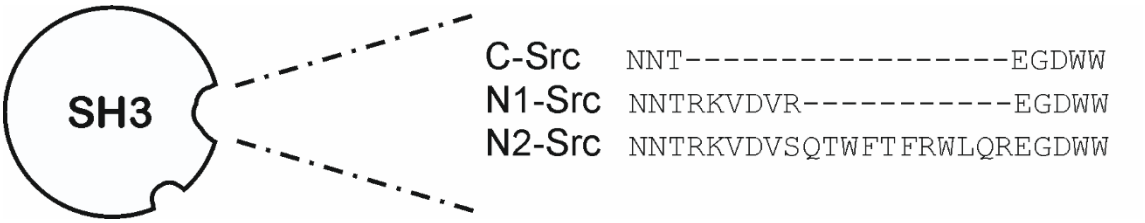

Figure 4. Splice variants of Src. Amino acid sequences of C-Src, N1-Src and N2-Src SH3 domains. The 6 amino acids of N1 microexon are found in N1-Src, while the total 17 amino acids of both N1 and N2 microexons are found in N2-Src.

Little is known about the functions of N1-Src, but it has often been linked with neuronal differentiation during development: for example, Maness and Aubry (1988) show by immunocytochemistry analysis that N1-Src localizes in neurite processes and growth cones and Cartwright et al. (1988) describe that high expression of N1-Src is concomitant with neurogenesis and neuronal growth during early stages of development. Another study by Kotani et al. (2007) related N1-Src function to the acquisition of neuronal morphology in Purkinje cells, as its overexpression caused deformities in microtubules and disrupted dendrite morphogenesis.

However, while the N1 neuronal splicing of C-Src is conserved from teleost fish to man, the N2-Src splice variant is only found in mammals, suggesting a role for higher brain functions (Collett and Steele 1992, Raulf, Robertson, and Schartl 1989, Yang et al. 1989).

1.4.2. N2-Src kinase

The inclusion of N1 and N2 mini-exons has significant consequences for the structure and thus the function and regulation of this kinase.

Through an *in vitro* assay, it was demonstrated that the autophosphorylation of Tyr 416 is higher in N2-Src than in C-Src (Keenan et al. 2015). This finding was confirmed in cells and at the same time it was also shown that the levels of phosphorylated Tyr 527 are much

lower for N2-Src, accounting for the increase in the kinase activity (Keenan et al. 2015). The increase in the kinase activity was then validated by the analysis of tyrosine phosphorylated proteins, which were more abundant in N2-Src overexpressing cells than in C-Src cells (Keenan et al. 2015). It has been hypothesized that the higher kinase activity seen in N2-Src could be dependent on an open conformation of the kinase, due to the diminished affinity of the SH3 domain for the SH2-kinase catalytic domain linker (Keenan et al. 2015).

Another difference that was found in N2-Src is a different affinity for SH3 ligand peptides, which determines distinct substrate specificity. It has been seen that C-Src phosphorylation of an ideal C-Src (Feng et al. 1995) substrate peptide is enhanced by the presence of a C-Src ligand (Feng et al. 1995), but not in the case of N2-Src (Keenan et al. 2015), thus meaning that the Pro-X-X-Pro motifs in target proteins could differ to those of C-Src. Indeed, a number of different proteins bind C-Src but not N2-Src, which led to the hypothesis that N2-Src is not just a constitutively activated form of C-Src, but a kinase with a distinct substrate specificity. It seems that the SH4 domain is not altered by the insertion of N1 and N2 microexons, therefore N2-Src could bind to membranes via myristoylation as in the case of C-Src.

Several papers show that a transcript high expression of N2-Src positively correlates with a favourable outcome for neuroblastoma patients (Mellstrom et al. 1987, Bjelfman et al. 1990, Matsunaga et al. 1993, Hedborg et al. 1995, Matsunaga et al. 1998). In particular, N2-Src has been associated with a less metastatic disease and a longer event free survival in patients (Matsunaga et al., 2000), link that was further confirmed in 2005 in a study by Terui et al. who correlated N2-Src with both a positive outcome. Strong evidences show that N2-Src may be favourably expressed in neuroblastomas discovered by mass screening, rather than by symptom (Matsunaga et al., 2000). These tumours are largely benign, with between 70 -90% being of favourable, stage I, II or the spontaneously regressing 4S and tend not to be Myc amplified (Bessho, 1998).

In 1993 Matsunaga et al. showed that a pattern of neuronal Src expression is matched by an ability to differentiate neuroblastoma cell lines under cAMP/Retinoic Acid. For example, they showed that SK-N-SH neuroblastoma cells have C-Src as the dominant isoform while N2-Src is entirely absent (Matsunaga et al., 1993). This data could suggest that a large number of N2-Src expressing neuroblastoma tumours are resolved without any treatment.

It has therefore been hypothesized that N2-Src kinase is able to induce differentiation in neuroblastoma cells, perhaps due to its higher kinase activity and different substrates in comparison to the ubiquitously expressed C-Src kinase. Indeed, preliminary data from the theses of previous research students in the Evans laboratory showed that this kinase is able to induce the extension of neurite-like processes in neuroblastoma cell lines (SK-N-AS and Kelly), even those that are retinoic acid-resistant, confirming the previously speculated role of N2-Src in the acquisition of neuronal morphology (Hernández Pérez 2015, Lewis 2014, Keenan et al. 2017). These data are the reason why N2-Src kinase was selected as the candidate to taken into further examination as a possible neuroblastoma differentiation strategy.

In work by Philip Lewis, HeLa cells stably transfected with N2-Src kinase were treated with and without sodium pervanadate, to inhibit endogenous protein tyrosine phosphatases (PTPs) and to activate Src family kinases, and were subjected to anti-phosphotyrosine immunoprecipitation. The immunoprecipitates (IP) eluates were processed by tandem mass spectrometry (MS/MS). The analysis involved quantitation (using emPAI) of peptide abundance between phosphotyrosine immunoprecipitations from control, C-Src and N2-Src HeLas. Therefore, peptides that were more abundant in the N2-Src sample represented proteins that were preferentially IP'd from N2-Src cells compared to C-Src and control. Consequently, the proteins that were enriched in the N2-Src IP were subjected to functional clustering of GO terms and interaction analysis by STRING.

This experiment suggested that N2-Src phosphorylates a significant functional cluster of protein members of the coat protein complex II (COPII), involved in endoplasmic reticulum (ER)-Golgi trafficking of secreted proteins (Lewis, 2014) (Fig.5).

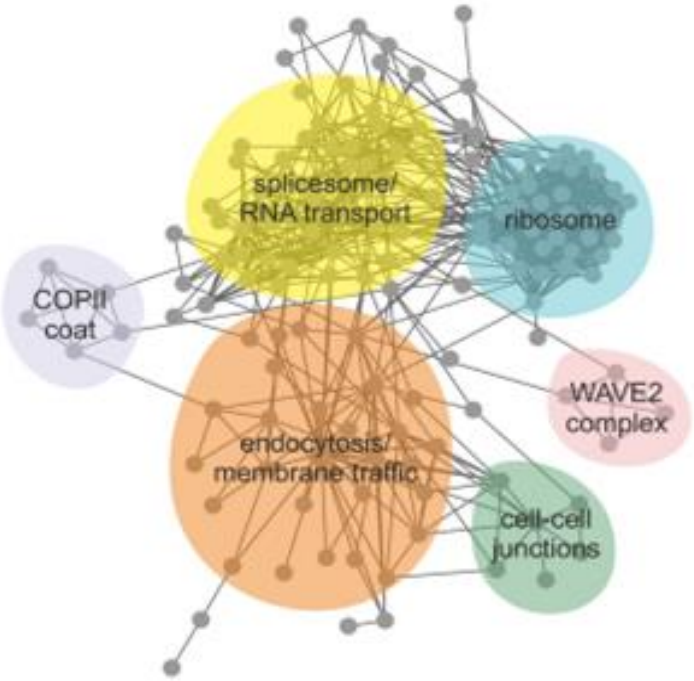

Figure 5. Functional clustering and interaction analysis. N2-Src HeLa cells were treated with and without sodium pervanadate and subjected to anti-phosphotyrosine immunoprecipitation. The IP eluates were processed by MS-MS and proteins that were enriched in the N2-Src IP were subjected to functional clustering of GO terms and interaction analysis by STRING (from Lewis 2014).

1.5. COPII trafficking

The COPII complex is a multi-subunit protein complex responsible for the formation of membrane vesicles at the ER destined for the *cis*-Golgi compartment (Fig. 6) (Barlowe et al. 1994). The coat comprises five subunits: the secretion associated, ras-related, GTPase (Sar1), the Sec23-Sec24 'inner coat' complex and the Sec13-Sec31 'outer coat' complex (Fig. 6).

Sar1 in its GTP-bound form binds to ER membranes and recruits the inner coat proteins (Nakano and Muramatsu 1989, Barlowe, d'Enfert, and Schekman 1993). Sec24 interacts with the cytoplasmic domains of cargo proteins (Fig. 6) and is primarily responsible for recruiting them for incorporation into vesicles (Miller et al. 2002, Miller et al. 2003, Mossessova, Bickford, and Goldberg 2003) but also Sec23 and Sar1 play a minor role in this process (Aridor et al. 2001, Giraudo and Maccioni 2003). The membrane-bound Sar1-Sec23-Sec24 complex recruits the Sec13-Sec31 outer coat (Salama, Yeung, and Schekman 1993, Aridor et al. 1998). The interaction between Sec23 and Sar1 results in stimulation of Sar1 GTPase activity through stabilization of GTP phosphate groups (Bi, Corpina, and Goldberg 2002) and the binding of Sec31 to Sec23 and Sar1 further enhance its GTPase activity (Antonny et al. 2001, Bi, Mancias, and Goldberg 2007). Therefore, full assembly of the coat

stimulates Sar1 GTP-hydrolysis activity (Antonny et al. 2001) and this enables the coat to depolymerize and be recycled for another round of vesicle biogenesis (Fig .6).

Although the five COPII coat proteins described above represent the minimal machinery required to bud a transport vesicle, there are additional factors that also participate, such as Sec16, a large multi-domain protein that associates peripherally with the ER membrane and is essential for ER export *in vivo* (Espenshade et al. 1995, Watson et al. 2006), and Sec12, a component that aids in the recruitment of Sar1 to the ER membrane through a GDP-GTP exchange (Fig.6).

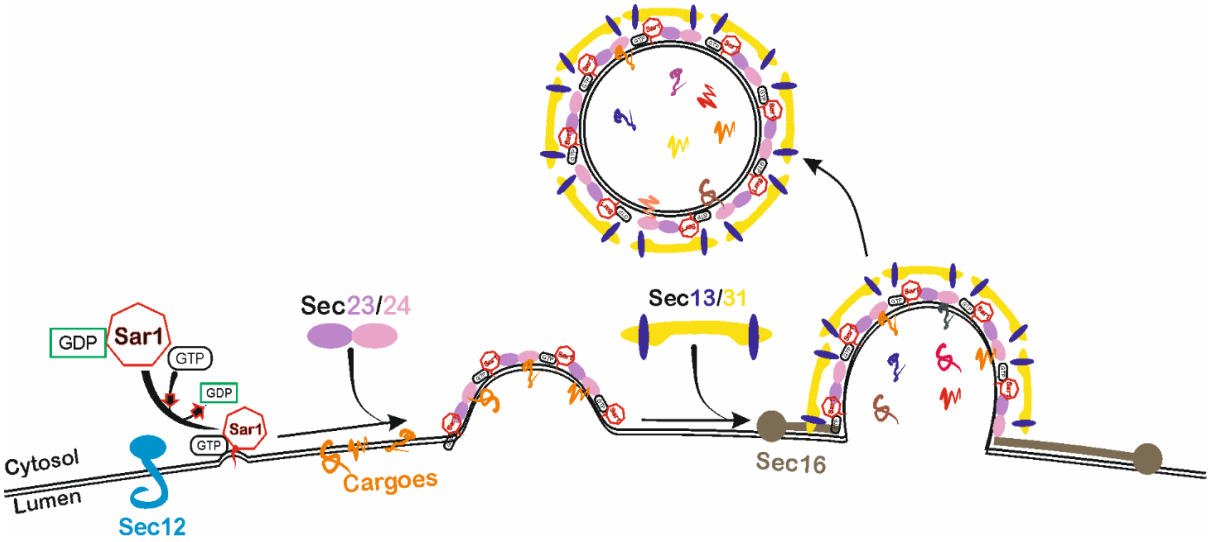

Figure 6. COPII vesicles formation. COPII coat formation at the ER is initiated by recruitment of Sar1 to the membrane in the GTP-bound state. Sar1-GTP recruits Sec23/24 heterodimer through interaction with Sec23 while Sec24 recruits cargo into pre-budding complexes. Sec13-31 complex is recruited to the inner coat layer through interactions with Sec23 and the coat drives membrane curvature, facilitating membrane deformation. Vesicle release from the ER is achieved in a manner related to Sar1 GTP hydrolysis. Sec12's aid in the recruitment of Sar1 and Sec16's scaffolding role are shown (adapted from D'Arcangelo, Stahmer, and Miller (2013)).

The putative interaction between N2-Src and COPII components, suggested by the aforementioned mass spectrometry analysis (Lewis 2014) and the fact that high expression of N2-Src correlates with a favourable outcome for neuroblastoma patients (Matsunaga et al. 1998), has led to the hypothesis that there could be an interplay between N2-Src and the COPII complex, which could be involved in neuroblastoma cell differentiation.

1.5.1. The COPII complex in neuronal differentiation

The importance and the role of the COPII components during neuronal differentiation has already been widely demonstrated: Sar1, Sec13, Sec31, Sec23 and Sec24 are transcriptionally upregulated to direct dendrite development (Iyer et al. 2013); Sar1 and Sec23 *Drosophila* homologues are necessary for correct dendritic growth and, if Sar1 is silenced, the transport of specific markers to the plasma membrane of dendrites is blocked (Ye et al. 2007); GABA transporter-1 axonal targeting requires Sec24 (Reiterer et al. 2008). Other studies have more broadly linked the secretory pathway to dendrite growth (Horton et al. 2005, Tang 2008, 2001) and in particular Horton et al. (2005) have shown how the polarization of secretory trafficking directs cargo for asymmetric neurite growth and morphogenesis. Moreover, the transport of phospho- and sphingolipid is extremely important in neuronal differentiation, as the protrusion of dendrites and axons requires a great amount of membrane (Lecuit and Pilot 2003), and the addition of membrane can be also achieved by exocytosis (Gauthier et al. 2009, Prager-Khoutorsky and Spira 2009). The mechanism of exocytosis is also used during the formation of axons and dendrites to deliver transmembrane and membrane-associated proteins, such as neurotransmitter receptors, adhesion proteins and axonal guidance proteins, to the outgrowing protrusions (Arimura and Kaibuchi 2007, Tang 2008, 2001).

Furthermore, the importance of COPII-dependent trafficking in neuronal differentiation can be fully appreciated, in particular, in the case of Sec23A deficiency. The Sec23A knockout mouse exhibits mid-embryonic mortality associated with the defective development of extraembryonic membranes and the re-opening of the neural tube in the midbrain area (Zhu et al. 2015). Furthermore, human Sec23A mutations cause the cranio-lenticulo-sutural dysplasia syndrome (CLSD), a disorder that is primarily characterized by late-closing fontanels, facial dysmorphisms, skeletal defects and sutural cataract, which links the biology of ER to Golgi trafficking with a clinical dysmorphology (Lang et al. 2006). The neuronal symptoms related to CLSD have not been fully explored yet, but Boyadjiev et al. (2011) reported a CLSD patient with seizures and neurodevelopmental delay. Moreover, it was demonstrated that Sec23A mice knockout show altered proliferation of neuroepithelium (Zhu et al. 2015).

Sec23A mutations also affect neuronal maturation by leading to an inhibition of dendrites and axon development. This data suggests that a dedicated role exists for the early secretory pathway in dendrites growth, but also in the axon growth, particularly under demanding conditions (Aridor and Fish 2009, Aridor et al. 2004, Ehlers 2007). Indeed, the study by Iyer et al. (2013) showed that CrebA can regulate high order dendritic branching complexity in *Drosophila melanogaster* through the COPII secretory pathway regulation. The overexpression of CrebA and the subsequent elevated levels of Sec31 or Sec23 may be capable of influencing the rate of COPII vesicle formation, which in turn could modulate dendrite development (Iyer et al. 2013). Furthermore, in a previous study conducted in Evans' laboratory by Hernández Pérez (2015), it was shown that Sec13 and Sec23A co-immunoprecipitate with N2-Src. In the same study, Sec23A was observed to be constitutively tyrosine phosphorylated in cells and the phosphorylation appeared to increase in the presence of N2-Src. No tyrosine phosphorylation of Sec13 in cells was detected under any condition. A preliminary experiment in the same study by Hernández Pérez (2015) showed that overexpression of Sec23A can inhibit the ability of N2-Src to differentiate SK-N-AS neuroblastoma cells.

Taken together, these data suggest a role for N2-Src in neurite-like process growth via the regulation of cytoskeletal and membrane dynamics, in particular through the interaction with members of the COPII complex. It was speculated that N2-Src binds Sec13 and phosphorylates Sec23A (Hernández Pérez 2015).

1.6. Aims

Based on the published and preliminary data described in this chapter, the central hypothesis of this study is that N2-Src regulates COPII transport to alter cell morphology and drive differentiation.

The hypothesis will be tested by addressing the following questions:

- Does N2-Src regulate COPII dependent secretion?
- Do N2-Src dependent effects on cell morphology require COPII?

Stable HeLa cell lines that inducibly express FLAG-tagged C-Src or N2-Src upon the addition of doxycycline were chosen as the model system for these experiments. In the absence of antibodies to N2-Src, these cells provided a robust system for comparing COPII traffic and cell behaviour in the presence and absence of N2-Src.

The migration and morphology of the cells was assayed by time-lapse microscopy and the inducible secretion of a fluorescent growth hormone cargo was used as a readout of COPII function. Finally, Sec23A shRNA constructs were developed and validated as tools to dissect the regulation of Sec23A by N2-Src in future experiments.

Addressing how N2-Src regulates COPII trafficking and modifies cell migration and morphology in a robust model cell line could then be used to gain further insights into neuroblastoma differentiation strategies.

2. Materials and methods

2.1. Materials

SYBR Safe was purchased from Life Technologies. Laemmli sample buffer was purchased from Sigma. Precision All Blue molecular weight markers were from Bio-Rad. Restriction enzymes XhoI and BglII were purchased from New English Biolabs (NEB). T4 DNA Ligase was purchased from Promega. The QIAquick Gel Extraction kit was purchased from (Qiagen) and the mini- and midi-prep kits from Machery-Nagel. Complementary oligonucleotides were from Integrated DNA Technologies (IDT). XL-10 Gold ultracompetent E coli were from Stratagene.

The following antibiotics were used: ampicillin (Melford), kanamycin (Sigma-Aldrich), penicillin/streptomycin (Gibco), doxycycline hyclate (Santa Cruz Biotechnology), hygromycin B. (Invitrogen). DMEM medium and FBS were purchased from Gibco, trypsin/EDTA from Invitrogen. Rapamycin was purchased from CELL guidance systems.

The following primary antibodies were used: mouse α-actin B antibody (Abcam), mouse α-FLAG (M2) (Sigma), mouse α-HA (Thermo Scientific), rabbit α-Sec23a (GeneTex), rabbit α-growth hormone (Insight Biotechnology), rabbit α-GFP (a generous gift from Dr. Paul Pryor, University of York). Secondary HRP conjugated α-mouse and α-rabbit antibodies were purchased from Sigma, Molecular Probes' secondary ALEXA fluor-conjugated antibodies were purchased from Invitrogen. Protein G agarose resin was purchased from GenScript. PVDF membrane (Immobilon-P) and the Immobilon chemiluminescent HRP substrate were purchased from Millipore and autoradiography film was from Santa Cruz.

Unless stated, all other reagents were purchased from Sigma-Aldrich.

2.2. Plasmids

The shRNA sequences to knock down Sec23A were found on the Broad Institute Portal (https://portals.broadinstitute.org/gpp/public/) and in a paper by Korpal et al. (2011) (Table 1). The correct insertion of the sequences into the plasmid vector was verified by sequencing (Genomics Lab, Technology Facility, University of York) with an M13reverse primer.

Clone ID	shRNA name	Sec23A target sequence	Match region
TRCN0000232510 (Broad Institute)	shRNA 1	ACCTAGTTATGCTGGTATATC (between nucleotide 285 and 305)	Coding sequence (CDS)
TRCN0000232509 (Broad Institute)	shRNA 2	ACGAGATGGAGTCCGATTTAG (between nucleotide 39 and 59)	CDS
TRCN0000232513 (Broad Institute)	shRNA 3	ATGACGGTTGTAACTACTAAA (between nucleotide 688 and 708)	3'UTR
KD#1 (Korpal et al. 2011)	shRNA 4	GCCTACAGCTTTGGTTGGACTT (between nucleotide 478 and 498)	CDS

Table 1. Oligo sequences and matching regions.

The pSUPER.mCherry/neo-shRNAs were created by substituting the EGFP open reading frame in the pSUPER vector with mCherry excised from pmCherry-N1 (Clontech). Mammalian expression plasmids encoding full length C- or N1-Src tagged at the C-terminus with FLAG or mCherry were previously described (Keenan et al. 2015). pC4S1-GFP-FM4-GH was a kind gift from Dr. Andrew Peden, University of Sheffield (Gordon et al. 2010).

2.3. Cell culture

Cells were maintained at 37 °C in a humidified atmosphere with 5 % CO2, in 25 cm^2 or 75 cm^2 Corning flasks with canted neck. Flp-in HeLa were cultured in DMEM (containing pyruvate, high glucose and glutamine (Gibco)) with 10% FCS and 1% penicillin/streptomycin (pen/strep).

Flp-in T-Rex HeLa cells stably expressing FLAG-tagged C- or N2-Src under the control of a tetracycline-inducible promoter were generated in the Evans lab by Dr Philip Lewis (Lewis 2014). Where appropriate, the parent Flp-in T-Rex HeLa line was used as a control. HeLa cells were cultured in 10% FCS and 1% pen/strep DMEM supplemented with 50 µg/ml hygromycin B to maintain selection of the Src-expressing cells.

Cells were passaged 2-3 times a week after reaching confluency. Passaging cells involved the removal of the culture medium, the washing of the cells with 10 ml of PBS and the addition of 1x trypsin/EDTA in PBS for 3 to 5 min. Trypsinization was halted by adding 5 or 10 ml of culture medium and cells were then centrifuged at 130 *g* for 5 min at 20 °C. The pellet was

resuspended in 1 ml of culture medium and split into flasks for passaging or quantified in a haemocytometer (Hawksley) for plating.

The cell lines used were checked by frequent DNA staining of live cells and were free of Mycoplasma spp.

2.4. Plasmid amplification and purification

2.4.1. Bacterial transformation

All transformations were performed using XL-10 Gold ultracompetent *E. coli.* 50 µl *E. coli* were transformed with 1-5 µg of plasmid DNA and incubated on ice for 30 min. They were then heat-shocked for exactly 45 s at 42 °C and incubated on ice for 2 min before adding 400 µl of LB medium (10 g tryptone, 10 g NaCl and 5 g yeast extract per litre) prewarmed to 42°C in a waterbath and incubated at 37 °C for 1 h at 200 rpm. 200 µl of cultured bacteria were plated on agar plates (10 g tryptone, 10 g NaCl, 5 g yeast extract and 20 g agar per litre) containing 100 µg/ml ampicillin or 50 µg/ml kanamycin, depending on the antibiotic selection of the plasmid, and incubated at 37 °C overnight.

2.4.2. Plasmid purification

Single colonies from the overnight bacterial transformation cultures were grown in selective LB medium at 37 °C overnight before lysis and plasmid purification using the Quick-Spin mini-prep kit or Midi-Prep kit as per the manufacturer's instructions. The identity of the plasmid was evaluated by performing a restriction digest followed by an agarose gel, with the uncut plasmid as a control, and its concentration was measured using a NanoDrop spectrophotometer (Technology Facility, University of York).

2.5. Transient transfection

The cells were plated 24 h prior to transfection (for the number of cells and the volumes used see Table 2) and the coverslips used for transfections in 24 well plates were sterilised in an oven at 180 °C for at least 30 min before use.

Cells were transfected using polyethylenimine (PEI), following the protocol described by Boussif et al. (1995). Briefly, DNA and PEI were diluted in serum free DMEM in different tubes (for the quantities see Table 2) and the two solutions were mixed and incubated for 20

min at room temperature to allow the formation of lipid-DNA complexes before pipetting drop-wise onto the culture medium in each well. After 5 h the medium was replaced with fresh medium, which contained 1 µg/ml doxycycline to induce expressions of C-Src or N2-Src HeLa. Cells were then fixed or lysed 24 h after transfection or 48 h for shRNA experiments. Control cells were transfected with empty plasmids and/or did not receive doxycycline treatment.

	Tissue culture dish	Coverslip	Cell number	Medium volume (µl)	DNA quantity (µg)	PEI volume (µl)
IC	24 well plate	Yes	5×10^4	0.5	1	3
WB	6 well plate	No	1×10^5	2	3	6
IP	100 mm dish	No	5×10^5	12	10	30

Table 2. Details for transient transfection protocols. Different tissue culture dishes were used for immunocytochemistry (IC), western blot (WB) and immunoprecipitation (IP) experiments. The type of culture dish that was used, the use of coverslips, the number of cells plated the day before transfection, the total volume of culture medium in which the cells were transfected and the quantity of DNA and reagent volume used per well/flask are specified for each type of experiment.

2.6. Immunocytochemistry

2.6.1. Cell fixation and staining

Cells were stained by immunocytochemistry after transfection or drug treatment and after being plated on 13 mm glass coverslips in a 24 well plate. The cells were washed three times in 1 ml PBS and then fixed for 20 min at room temperature in 0.5 ml paraformaldehyde (4% paraformaldehyde and 4% sucrose in PBS, pH 7.4). The cells were then washed three times in PBS and permeabilised for 30 min in PBS + 1% BSA + 0.1% Triton X-100. The cells were then incubated with α-FLAG (M2) primary antibody in 1% BSA in PBS in a dilution of 1:3000 for 2 h at 37 °C in a humidified atmosphere. The cells were then washed three times in 1 ml PBS before application of the α-mouse ALEXA 594 secondary antibody in PBS + 1% BSA in a dilution of 1:500 for 1 h in the dark at room temperature. The coverslips were finally washed three times in 1 ml PBS and once with dH_2O and air-dried prior to mounting on microscopy slides

using Mowial (10% Mowial, 25% glycerol in 0.1 M Tris pH 8.5, containing 1 µg/ml DAPI). Cells transfected with GFP plasmids alone were mounted on microscope slides immediately after fixing. Some coverslips were incubated with the secondary antibody alone, in order to control for non-specific staining.

2.7. Microscopy and image analysis

2.7.1. Fluorescence imaging

Images were acquired with the digital camera using a Leica AF600 epifluorescence microscope with a 100x objective (Technology Facility, Department of Biology, University of York).

The quantitative analysis of the number of vesicles was performed using the ImageJ Squassh plug-in described in **2.7.2**.

2.7.2. "Squassh" segmentation method

To analyse the changes in the number of the ER secreted vesicles, the HeLa cells that were transfected with the pc4s1-GFP-FM4-GH plasmid were stained and the images were acquired with a Leica AF600 fluorescent microscope. To segment and quantify the number of vesicles for each condition and at each time point, I employed the Squassh plug-in for Image J and the protocol described by Rizk et al. (2014)

This software exploits a segmentation method that is able to connect the segmentation task with the biological reality using information about the imaged objects, the process of the picture formation and the background noise in the image (Rizk et al. 2014). Moreover, this method of segmentation reduces the chance of bias by combining image de-noising, deconvolution and segmentation, without separating the de-noising or the deconvolution of the images beforehand (Paul, Cardinale, and Sbalzarini 2013).

The procedure, described by Rizk et al. (2014), starts with the background subtraction, based on a rolling ball algorithm (Sternberg 1983), in order to reduce excess fluorescence. The plugin requires to enter a 'rolling ball window size', which defines a square with sides of a length that would not fit within the objects to be detected. The size chosen allows the plugin algorithm to analyse intensity histograms in a window that moves across the picture like a 'rolling ball', in order to recognize the most frequently occurring intensity value as the local background estimate. To identify each single fluorescent vesicle spreading from the ER, it was chosen a rolling ball size of 10 pixels (Fig. 7).

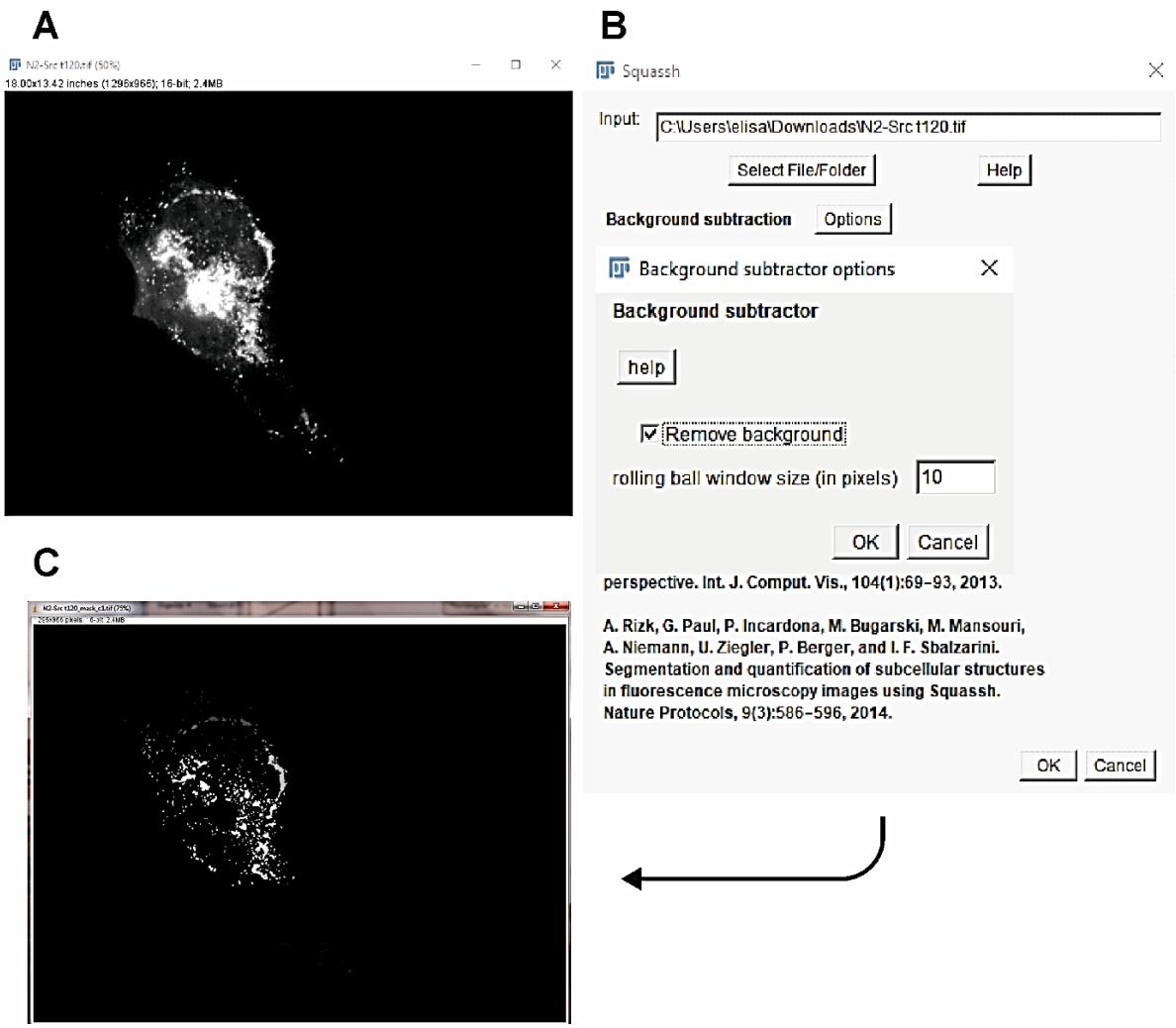

Figure 7. Illustration of the procedure's steps used to analyse the cell vesicles using the ImageJ plugin "Squassh": background subtraction. In order to reduce the fluorescence excess, the plugin requires to enter the rolling ball window size so that a square with that edge length would not fit in the objects to be detected.The next step involved the segmentation parameters: it starts by setting the regularization parameter, in order to avoid segmenting noise-induced small intensity peaks (the value chosen was 0.05). It then requires a value for the minimum object intensity channel (the set value for this analysis was 0.150), in order to increase the sensitivity during the segmentation process; the plugin also requires setting the noise model corresponding to the

microscope and detector used, which in the case of a wide-field microscope used to obtain the pictures is a Gaussian model. Finally, the information about the microscope point spread function (PSF) are set and these can be either theoretical (which is provided by the software for the wide-field microscope, the one used for this experiment) or a measured one (Fig. 8).

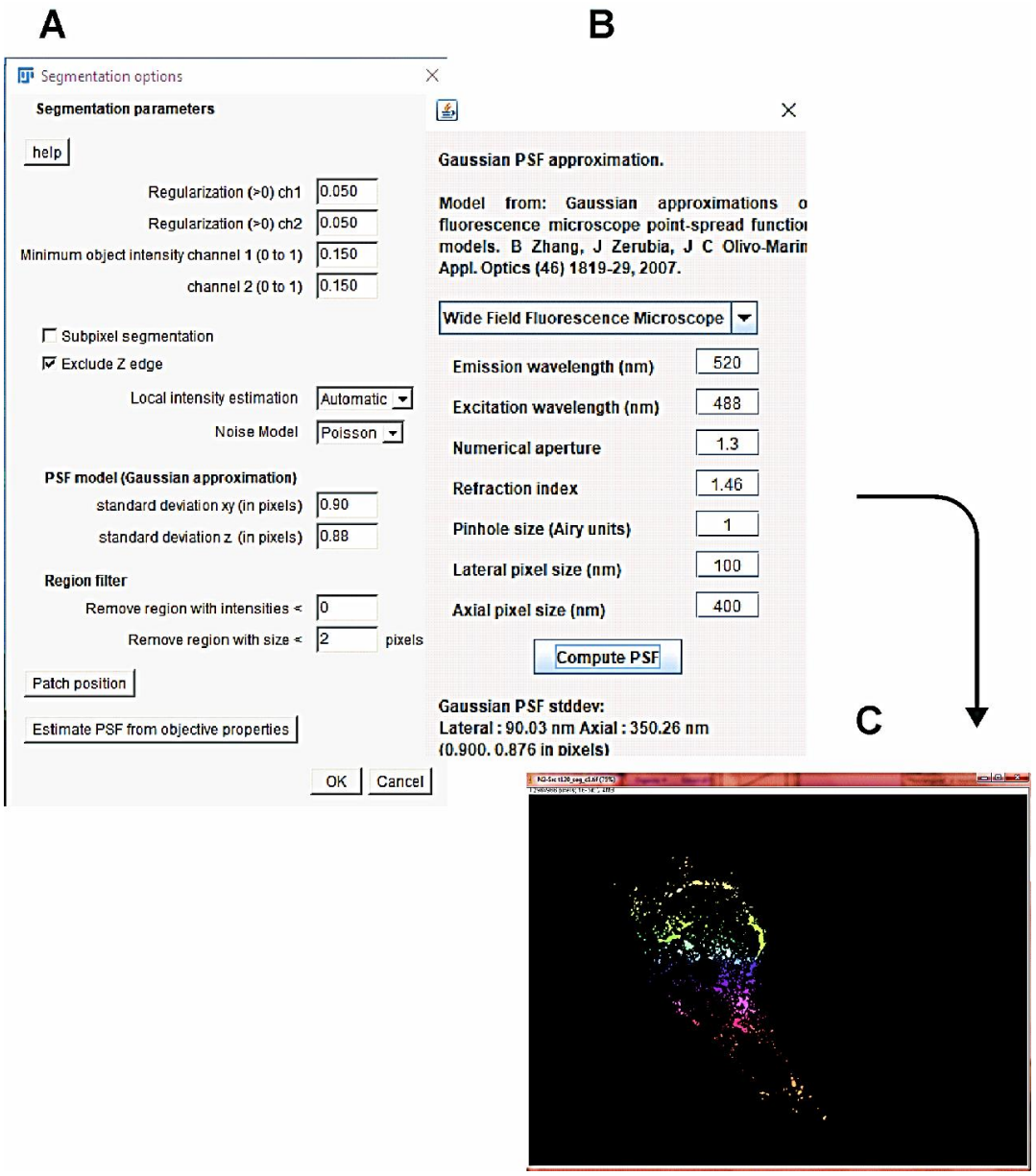

Figure 8. Illustration of the procedure's steps used to analyse the cell vesicles using the ImageJ plugin "Squassh": segmentation parameters. It directly connects the segmentation process with the biological reality, by entering parameters like the microscope PSF, the regularization parameter and the threshold, to avoid segmenting noise-induced small intensity peaks and for the minimum object intensity to be considered.

It is also possible to select an output which contains the 'intermediate steps' (as shown in Fig. 7 and 8), the 'object intensities', which displays the objects in their estimated fluorescence intensities (Fig. 9B), and the 'object outlines', that show an overlay of the original

image with the segmented outline (Fig. 9C). It is also possible to select 'save object and image characteristics' to store the quantifications in .csv files, that were used to obtain the number of vesicles per picture (Fig. 9D).

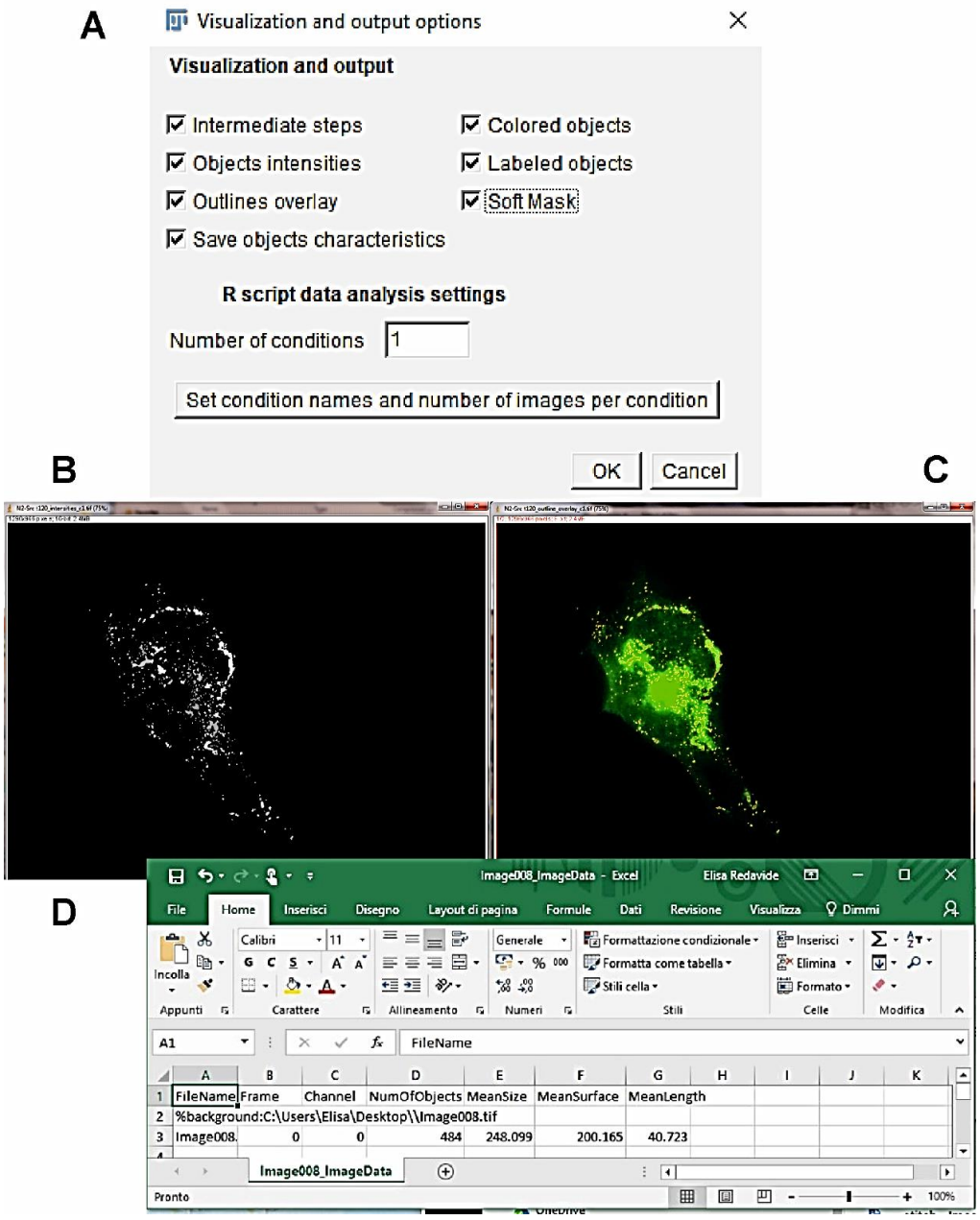

Figure 9. Illustration of the procedure's steps used to analyse the cell vesicles using the ImageJ plugin "Squassh": visualization and output options. The plugin allows to select how to visualize the result of the segmentation, like the .cvs file which contains the resulting object quantifications, or the pictures of the object intensities or the object outlines, to visualize the estimated fluorescence intensities of the objects or the overlay of the original image with the segmented outlines.

The number of vesicles per cell for each picture at each time point (circa 20 cells per time point and per condition) was then carefully analysed and the median was calculated.

2.7.3. Ptychography

To address the effects of N2-Src on cell migration and morphology the Phasefocus Virtual Lens® technology was used. This is a new technique with a 'lensless' imaging method, that has the advantage of having no associated lens-related aberrations or limitations. The Phasefocus technology was integrated with a conventional microscope for conventional imaging, but also for optical and geometric flexibility.

Flp-in T-Rex HeLa and stable C-Src and N2-Src Flp-In-T-Rex HeLa cells were plated on a 6 well plate at a confluency of 20% 24 h prior to imaging for the free migration assay, while for the wound healing assay stable C-Src and N2-Src Flp-In-T-Rex HeLa cells were plated on a 6 well at a confluency of 100% always 24 h prior to imaging. Where appropriate, cross-shaped wounds were introduced using a yellow pipette tip drawn through the cells in two perpendicular lines. Time-lapse imaging was performed by placing the 6 well plate in the chamber slide on the VL21 microscope and the microscope and the cells were maintained at 5 % CO_2 and 37°C.

For the random migration assay, images were acquired by sequentially visiting the 3 wells with a 10x objective with a time of 7.5 min between imaging the same well. The region of interest (ROI) for each well, one ROI per well, was 1.03x1.03 mm. Doxycycline (1 µg/ml) was added to all wells to induce the expression of C-Src-FLAG and N2-Src-FLAG and the pictures were acquired for 48 h. Doxycycline was added to the Flp-in Hela well too, in order to use it as a control.

For the wound healing assay, doxycycline was added to the wells 24 h before the cross-shaped wounds were introduced and images were acquired by sequentially visiting the 4 wells with a 10x objective with a time of 11.3 minutes between imaging the same well. The ROI for each well, two ROIs per well, was 0.83 x 1.66 mm. C-Src and N2-Src Hela cells without the addition of doxycycline were used as a control.

The data were then segmented using the Cell Analysis Toolbox (CAT) automated cell tracking software. The segmentation default 'recipe' was adjusted to remove the background and allow the software to identify the exact morphology of the cells to track (Godden et al. 2014, O'Toole and Suman 2014). In order to get an understanding of the kinetic behaviour of each different cell for each cell line, the data were then exported by single cell tracking. Indeed, the CAT software is able to track each individual cell over time and identify changes

in migration and morphological behaviour: it was therefore possible to individualize each cell in the ROI, assigning it with an ID and following the kinetic behaviour and morphology over the time course experiment.

2.7.4. Wound healing assay analysis

To measure the area migrated in a wound healing assay, the multi-image TIF acquired with a 10x microscope was analysed in ImageJ. The percentage decrease of the wound area over 48 h was analysed by outlining the wound on the first image of the time-course using the polygon tool, then again outlining it at T24 h and at last on the final image of the time-course and the area of the wound between these outlines was measured by ImageJ. The data for these time-courses was then exported and analysed in Microsoft Excel.

2.8. Immunoprecipitation

Cells plated in 10 cm dishes were washed three time with PBS, before the addition of 800 µl of RIPA buffer (10 mM Tris-HCl, pH 7.4, 1 mM EDTA, 0.5 mM EGTA, 1% Triton X-100, 0.1% sodium deoxycholate, 0.1% SDS, 140 mM NaCl) containing 0.1% β-mercaptoethanol, 0.1% protease inhibitors and 1 mM sodium orthovanadate. Both the buffers and samples were kept on ice during the whole process. The cells were scraped from the bottom of the dishes using a cell scraper, transferred to an Eppendorf tube and incubated on ice for 10 min at 4 °C to remove the insoluble fraction. The lysates were spun at 16,000 g for 10 min at 4 °C to remove the insoluble fraction and a Bradford assay was performed to determine the protein concentration and to allow equal amounts of proteins to be used for each sample (1 mg/ml). 100 µl of the lysate was kept as 'input' and the 700 µl of lysate left were incubated with 3 µl of HA antibody overnight on a rotating wheel at 4 °C. Fifteen µl of protein G beads were then added for another hour of incubation at 4 °C on a rotating wheel to recover the immune complexes, the beads were then pelleted for 5 min at 4 °C at 720 g and the supernatant was collected to assess the IP efficiency. The beads were resuspended in 0.5 ml of PBS and the washing and elution steps were performed using 0.45 µm filter spin columns (Spin-X, Costar), which were previously washed twice in PBS. The beads were washed three times in 500 µl PBS by pulsing for 30 s in a microcentrifuge at 4 °C and, to elute the complex of interest, 30 µl of 2x Laemmli buffer was added to the filter tubes and incubated for 10 min on a rocking

platform at room temperature. The tubes were finally centrifuged for 10 min at 16,000 g and the eluate stored at -20°C.

2.9. SDS-PAGE and Western blotting

2.9.1. SDS-PAGE

Samples were either lysed directly into 2x Laemmli loading buffer or diluted in 2x Laemmli loading buffer, then boiled at 95 °C for 10 minutes prior to loading.

Proteins were separated using the sodium dodecyl sulphate polyacrylamide gel electrophoresis (SDS-PAGE). The gels were composed of a resolving gel (375 mM Tris-HCl pH 8.8, 0.1% SDS, 10 % acrylamide/bisacrylamide, 0.05% APS, 0.01% TEMED in dH_2O) and a stacking gel (125 mM Tris-HCl pH 6.8, 0.1% SDS, 4% acrylamide, 0.05% APS, 0.01% TEMED in dH_2O).

The samples were loaded into the gels immersed in 1X SDS running buffer (250 mM Tris, 1.92 M glycine, 1 % SDS in dH_2O) and run at 190 V until the pre-stained protein molecular weight marker (Bio-Rad) reached sufficient resolution of the target protein size.

2.9.2. Protein transfer

Proteins were transferred from SDS-PAGE to polyvinylidene difluoride (PVDF) membranes. First, the PVDF membrane was activated in 100 % ethanol for at least 1 minute and then equilibrated along with the gel in transfer buffer (25 mM Tris, 190 mM glycine, 20 % methanol). The gel and the membrane were placed in the cassette between two pieces of 3MM paper (Millipore) and pads soaked in transfer buffer.

The assembly was placed in the transfer cell and the transfer was performed at 67 V for one hour. At the end of the transfer, the membrane was stained with Ponceau red (0.1% Ponceau S, 5% acetic acid in dH_2O) to confirm the correct transfer of proteins.

2.9.3. Western blotting

All incubations were performed on a rocking platform. The PVDF membrane was washed in water and PBS before being blocked for one hour in PBS supplemented with 3% skimmed milk at room temperature. The PVDF membrane was then probed with primary antibodies (Table 3) overnight at 4 °C or for 2 h at room temperature and then the membrane was washed three

times for 5 min in PBS Tween (PBS + 0.5% Tween-20). The membrane was incubated for 1 h at room temperature with an HRP conjugated secondary antibody diluted in PBS + 0.5% Tween and 3% skimmed milk and then it was washed three times for 10 min in PBS + 0.5% Tween and incubated for 1 min with chemiluminescent HRP Substrate before visualising bands in a darkroom using autoradiography film. Exposure times were variable and ranged from 10 s to 20 min, depending on the intensity of the signal.

To strip a membrane for reprobing with a different antibody, it was incubated three times for 10 min at room temperature with stripping buffer (136 mM NaCl, 20 mM glycine, pH 2.5) and washed three times in dH_2O and then three times in PBS.

When appropriate, the intensity of the bands was quantified by densitometry using ImageJ.

Primary Antibody		**Secondary Antibody**	
Antibody	**Concentration**	**Antibody**	**Concentration**
α -FLAG	1:500	α-mouse IgG HRP	1:5000
α-Sec23A	1:1000	α-rabbit IgG HRP	1:5000
α-HA	1:500	α-mouse IgG HRP	1:5000
α-actin B	1:1000-3000	α-mouse IgG HRP	1:5000
α-GH	1:700	α-rabbit IgG HRP	1:5000
α-GFP	1:10000	α-rabbit IgG HRP	1:5000

Table 3. Western blot antibodies and dilutions. Antibodies used for protein labelling in Western blotting experiments and their correspondent secondary antibody. Dilution was made in PBS for primary antibodies and in PBS + 3% milk + 0.5% Tween-20 for secondary antibodies.

2.10. Statistical analysis

The number of biological replicates was insufficient to perform any statistical analysis, but in the experiments in which the n=2 showed a trend that should be confirmed by further experiments in order to confirm these interesting preliminary data.

3. Results

3.1. Src kinases expression in inducible cell lines

To gain better insight into the interaction between COPII traffic and cell behaviour in the presence and absence of N2-Src, HeLa cell lines that inducibly express FLAG-tagged C-Src or N2-Src upon the addition of doxycycline were chosen as the model system.

I first verified that the Flp-in HeLa cell lines stably transfected with C-Src or N2-Src kinase exhibited doxycycline-dependent expression (Fig. 10A). As shown in Figure 10B and 10C, in the presence of doxycycline, the expression of C-Src and N2-Src kinases is detectable by Western blotting at 6 h, it plateaus at 9-24 h, and it reaches the maximum expression at48 h.

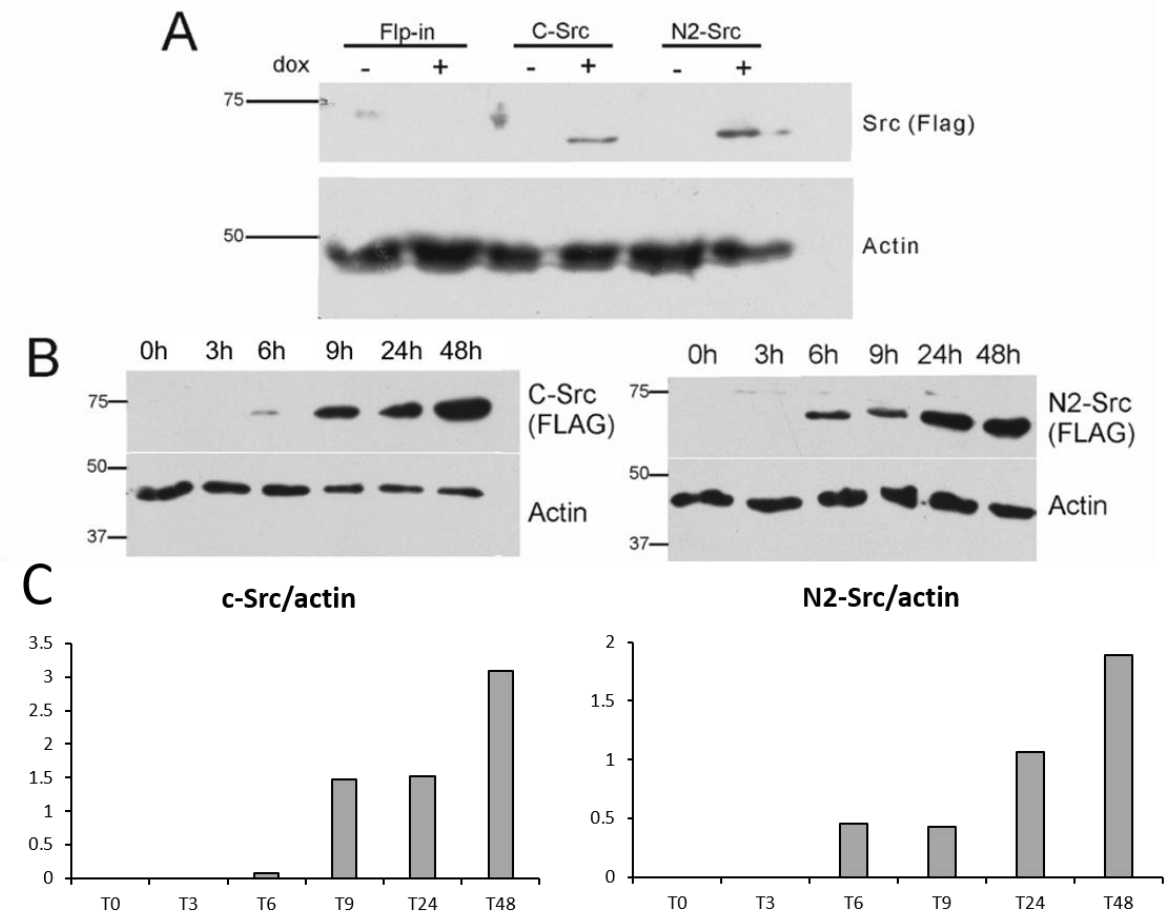

Figure 10. Inducible and time dependent expression of Srcs in Flp-in HeLa cell lines. (A) Control, C-Src or N2-Src expressing HeLa cells were lysed 24 h after the addition of doxycycline (1 µg/ml) and separated by SDS PAGE. The gel was immunoblotted for FLAG and actin. (B) C-Src or N2-Src Flp-In HeLa

cells were lysed at the indicated times after the addition of doxycycline and the samples were then run on a SDS PAGE, prior to immunoblotting with α-FLAG and α-actin. (C) c-Src and N2-Src relative protein expression compared to the actin loading control. The expression of the proteins of interest is detectable by Western blotting at 6 h, it plateaus at 9-24 h, and it reaches the maximum expression at48 h.

3.2. Src kinases decreases migration in a wound healing assay

As previously demonstrated in a preliminary experiment by Lewis (2014), the inducible expression of N2-Src kinase is able to decrease migration and proliferation in a wound-healing assay. The wound healing assay is an assay that involves an artificial mechanical scratch on a confluent cell monolayer that scrapes off an area covered by cells (Rodriguez, Wu, and Guan 2005). Cells are then stimulated by the availability of empty space (Poujade et al. 2007) and the ones at the edges of the scratch proliferate and move toward the centre of the wound area until it is closed (Ascione et al. 2016). To confirm and extend the results obtained by Lewis (2014), ptychography was used to gain a better characterisation of cell migration and proliferation in a random migration assay. In this study, a Phasefocus ptychography system was used (Marrison et al. 2013). Ptychography uses Coherent Diffractive Imaging (CDI) to reconstruct a target object from the diffraction pattern it generates when illuminated by a source (Maiden and Rodenburg 2009). It can be applied to visible light microscopy to produce high resolution quantitative phase images of low-contrast objects, such as unlabelled cells, and it works also in transmitted and reflected light applications (Maiden and Rodenburg 2009). The Phasefocus data can then be used to measure parameters of interest, depending upon the specimen and the wavelength used.

C-Src Hela and N2-Src HeLa cell lines were plated at 100% confluency in a 6 well plate in duplicate and 6 h after being plated, doxycycline was added to one C-Src well and one N2-Src well. The following day a cross-shaped scratch was applied to all of the wells and the cells were imaged approximately every 11 min for 48 h with the Phasefocus technology with a 10X magnification. There were two rectangular ROIs for each well, measuring 0.83 x 1.66 mm. The experiment was repeated twice.

Representative Phasefocus pictures of the different cell lines at the different time points analysed with and without the addition of doxycycline are shown in Fig. 11 and Fig. 12.

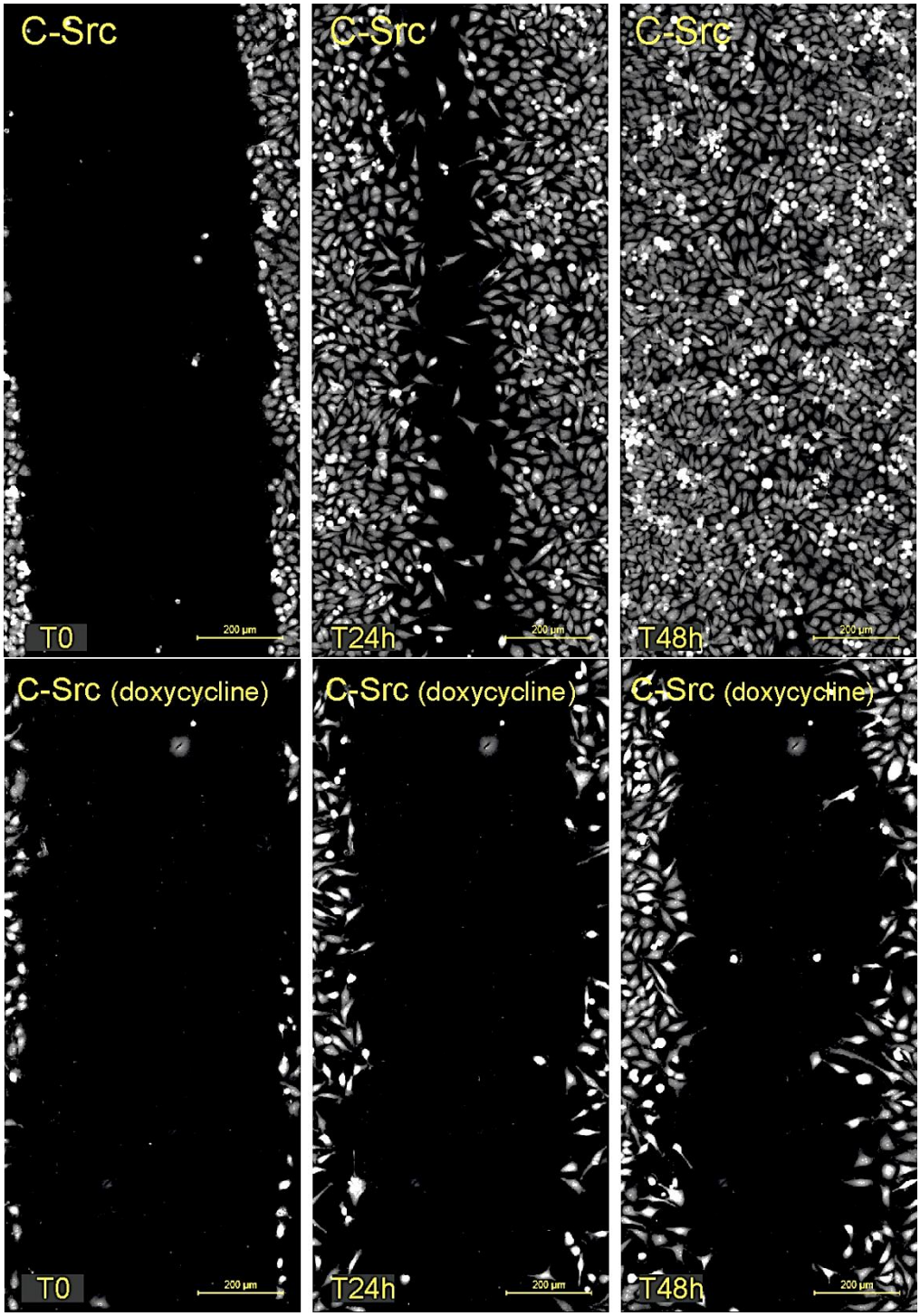

<u>Figure 11.</u> Representative Phasefocus picture of the C-Src cell line at the different time points analysed during the first biological replicate of the wound healing assay, with and without the addition of doxycycline to induce the expression of C-Src kinase.

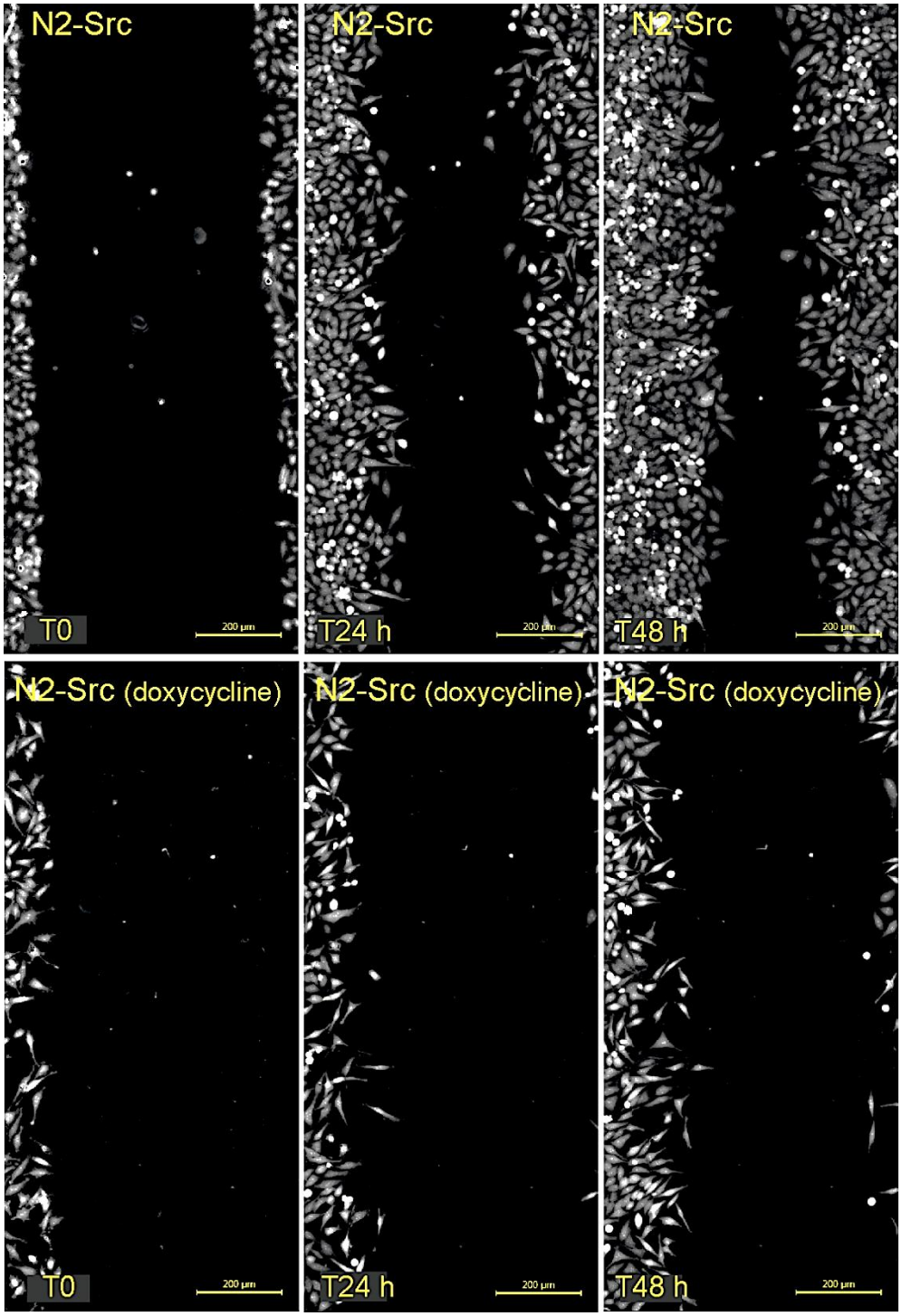

<u>Figure 12.</u> Representative Phasefocus picture of the N2-Src cell line at the different time points analysed during the first biological replicate of the wound healing assay, with and without the addition of doxycycline to induce the expression of N2-Src kinase.

As it can be seen from Fig. 11 and Fig. 12 (top pictures), untreated C-Src cells can migrate to completely fill the wound area in 48 h, whereas N2-Src cells did not: this may suggest either a leaky expression of the N2-Src kinase or fundamental differences in cell behaviour between

these two cell lines that should be further analysed. As far as it concerns the treated cell lines (Fig.11 and Fig 12, bottom pictures), it can be seen that the addition of doxycycline profoundly affects the migration of C-Src cells, whereas the effect on the N2-Src ones seems less profound. Overall, the N2-Src cells treated with doxycycline, used to induce the expression of the kinase in analysis, migrated less into the wound over the 48 h.

To gain a better understanding on the decrease of the wound area the Phasefocus time lapse pictures were analysed with ImageJ software. Fig. 13A shows the quantification of the mean change in % wound area. It is possible to see a trend in which the C-Src cells receiving the doxycycline treatment were able to decrease the wound area more in both the experiments, compared to the N2-Src cells that were treated with doxycycline. Indeed, this trend showing the % wound area decrease was greatest at 24-48 h. Interestingly there was a high proliferative activity even in the C-Src cell line that did not receive the doxycycline, in particularly in the first 24 h after the scratch, compared to the N2-Src cell line that did not receive the doxycycline either. However, the difference between the untreated C-Src and N2-Src cells decreases at the time point 24-48 h, where they have a similarly percentage decrease of the wound area (Fig. 13).

Moreover, by exploiting the Phasefocus technology and the subsequent CAT analysis software, it was feasible to analyse the track length of every single cell present in the selected ROI. It was observed a trend that the doxycycline treatment increased the median track length in C-Src cells. However, when N2-Src expression was elicited by the doxycycline treatment, the median track length did not change over the 48 h in which the cell lines were imaged (Fig 13B).

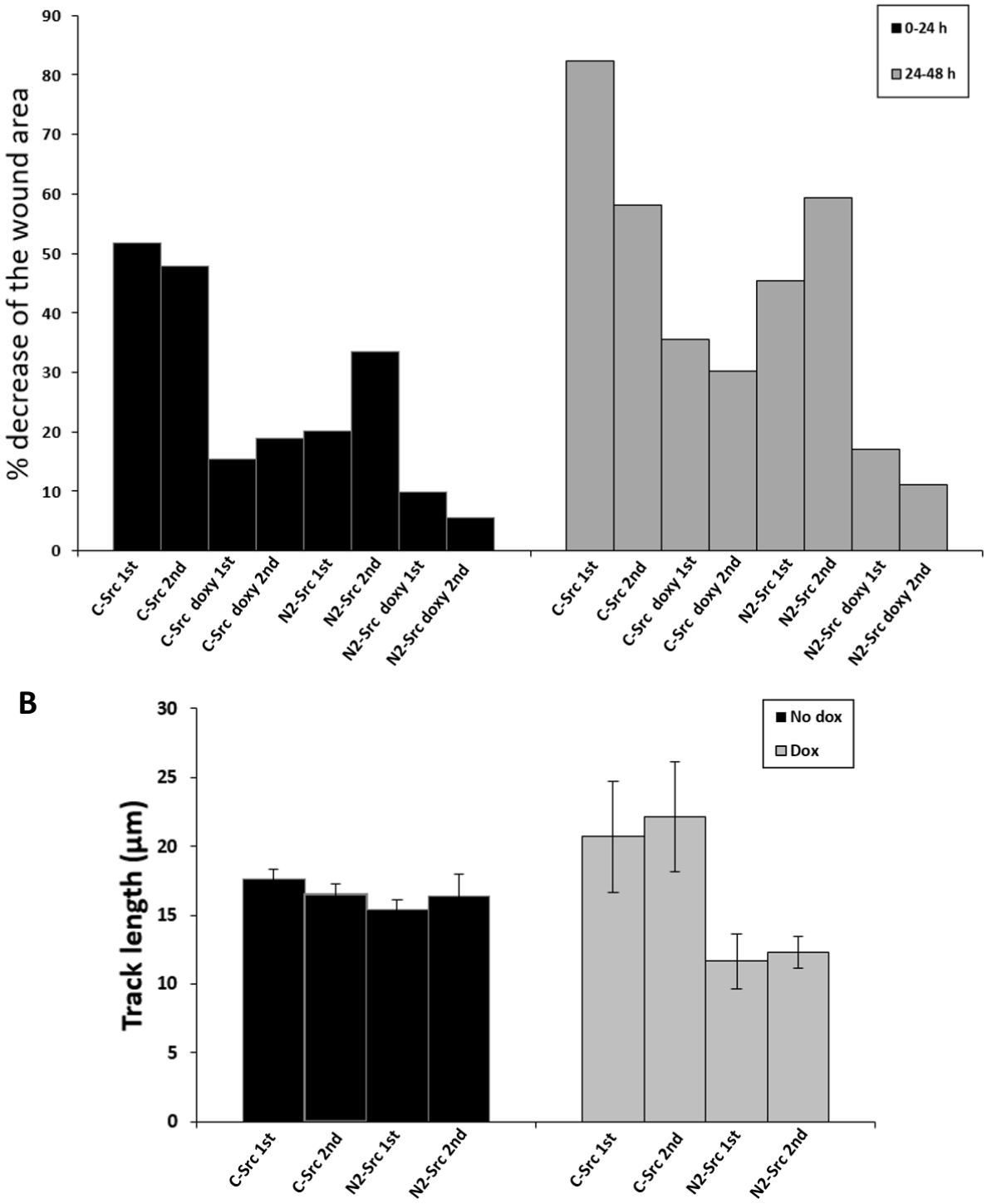

Figure 13. N2-Src expressing cells have reduced cell migration compared to C-Src cells in a wound healing assay. C-Src and N2-Src Flp-In HeLa cells cultured in a 6 well plate, in medium containing doxycycline or vector to induce the expression of Src kinases, were mounted in the environmental chamber (37°C, 5% CO_2) of the Phasefocus microscope. Images were acquired every 11.3 min for 48 h after the wound, with a ROI size of 0.83 x 1.66 mm. (A) The polygon tool in ImageJ was used to measure the area of the wound at 0, 24 and 48 h. The data are plotted as the difference in % coverage of the ROI by the wound for the indicated time ranges. (B) The track length of each cell was calculated using the CAT segmentation software. Data are plotted as the median of the single cell track length (µm), with the error bar showing the standard error of the median. The data are from the analysis of an average of 3000 cells per cell line and treatment from two independent experiments.

3.3. Src kinases decreases migration in a random migration assay

To expand on the findings in the wound healing assay, it was chosen to analyse the cell migrating and proliferative behaviour in a random migration assay. In this assay, cells do not have external clues and simply explore their local environment, whereas during the wound-healing assay the cells at the edge of the wound undertake directed migration until new cell–cell contacts are established again (Poujade et al. 2007, Liang, Park, and Guan 2007, Jonkman et al. 2014). The Flp-in HeLa cell line (used as a control) and the C-Src and N2-Src expressing cell lines were plated at a confluency of 20% in a 6 well plate. The following day doxycycline was added to the medium and images were acquired every 7.5 min for 48 h with the Phasefocus microscope at 10X magnification. The region of interest for each well was 1.03 x 1.03 mm.

A representative Phasefocus image of the cell lines at the different time points analysed after the addition of doxycycline is shown in Fig.14.

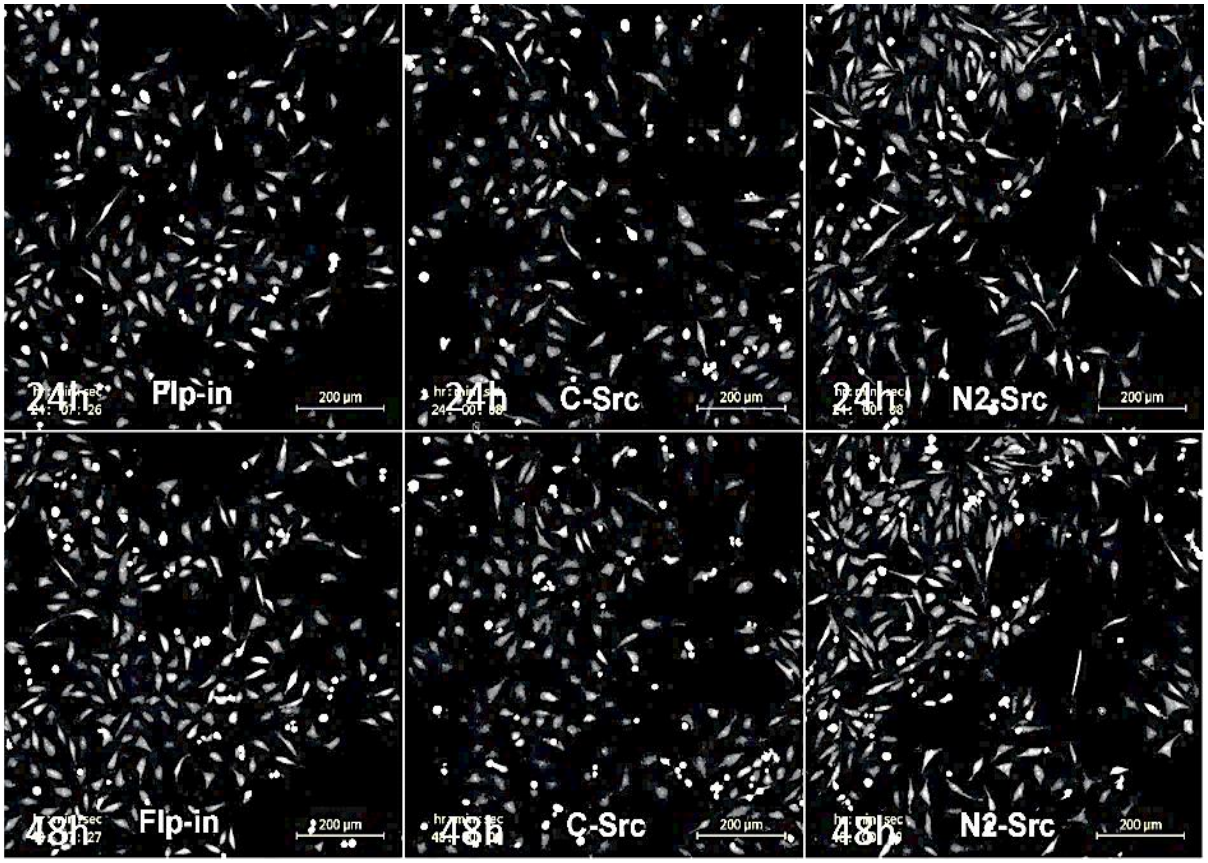

<u>Figure 14.</u> Representative Phasefocus picture of the cell lines at the different time points analysed during the random migration assay, after the addition of doxycycline to induce the expression of Src kinases.

The tracking data of individual cells obtained were exported from the CAT software and the median track length (in µm) was calculated. As shown in Figure 15A, the N2-Src cells show a decrease in the median track length after the addition of doxycycline, both after 24 h and 48 h, compared to the Flp-in HeLa and C-Src HeLa. Surprisingly, the Flp-in control cells had an increased track length in the second 24 h following doxycycline treatment. Moreover, Fig. 15B shows that the percentage of doxycycline treated N2-Src cells that showed no movement at all was almost 18% compared to approximately 11-12% in the other cell lines.

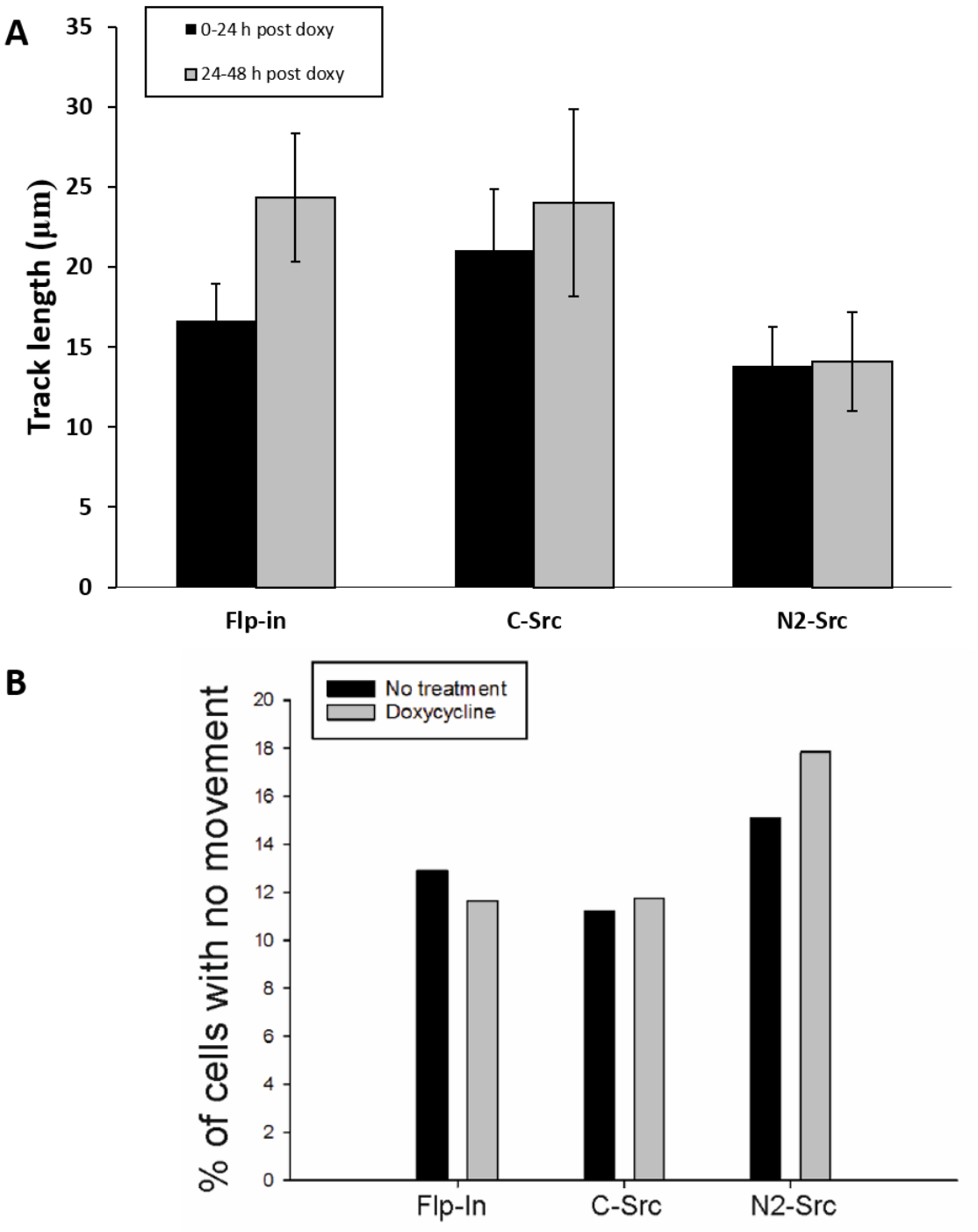

Figure 15. N2-Src reduces cell migration in a random migration assay. Control, C-Src and N2-Src Flp-In HeLa cells cultured in a 6 well plate were mounted in the environmental chamber (37°C, 5% CO_2) of the Phasefocus microscope and observed for 48 h following the addition of doxycycline. Images were acquired every 7.5 min, with a ROI size of 1.03x1.03 mm, and the track length of each cell was calculated using the CAT segmentation software. (A) Data are plotted as the median of the single cell track length (µm), with the error bar showing the standard error of the median. (B) The number of cells that had a track length of zero was divided by the total number of cells analysed by the CAT segmentation software to obtain the percentage of cells that did not move over the 48 h of observation. The data are from an average of 1500 cells per cell line, from 1 well per condition analysed from a single experiment.

3.4. N2-Src redistributes and increases the number of secretory vesicles

Neurite or neurite-like process outgrowth, is a mechanism that requires the addition of plasma membrane, which is provided by exocytosis of secretory vesicles (Gauthier et al. 2009, Prager-Khoutorsky and Spira 2009). I therefore hypothesised that regulation of COPII transport by N2-Src might increase the rate of secretion to provide sufficient lipids for the membrane dynamics necessary for neuronal differentiation. To observe and measure the effect of N2-Src on COPII-dependent secretion, I employed a plasmid encoding a fluorescent secretory cargo (kindly provided by Andrew Peden, University of Sheffield) that accumulates in the ER and can be induced to secrete by the addition of rapamycin.

The Peden lab modified the reporter construct included in the Ariad RPD Regulated Secretion/Aggregation Kit (Ariad Pharmaceuticals) by adding an N-terminal green fluorescent protein (eGFP) tag downstream of the signal sequence, to obtain a pc4s1-GFP-FM4-GH plasmid (Fig. 16, from Gordon et al. 2010).

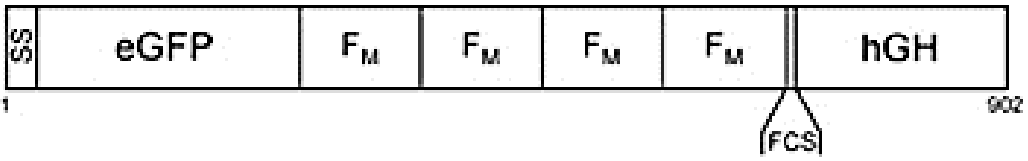

Figure 16. Schematic of the reporter construct used to measure secretion. SS, signal sequence; eGFP, enhanced green fluorescent protein; FM, FKBP mutated; FCS, furin cleavage sequence; hGH, human growth hormone; numbers represent amino acids (from Gordon et al. 2010)

This construct is based on a "reverse dimerization" system (Rollins et al. 2000) in which aggregation is the resting state and the ligand breaks up protein-protein interactions. This system contains a conditional aggregation domain that self-aggregates, but the constitutive aggregation can be blocked by rapamycin, allowing for the signal sequence to drive secretion and the FCS to release the soluble GH in response to the ligand.

The conditional aggregation domain is based around the property of mutant FK506-binding protein (FKBP) to form ligand-reversible dimers. FKBPs belong to the immunophilin family and are involved in several biochemical processes including protein folding, receptor signalling, protein trafficking and transcription (Kang et al. 2008). A single mutation (F36M) allows the usually monomeric FKBP proteins to become ligand reversible dimers. When

mutant FKBPs are linked together, they aggregate so that when expressed in the ER they cannot be secreted. If cells are incubated with rapamycin, the ligand that normally induces FKBP dimerization, being a reverse dimerization system, the aggregates solubilize and the construct is secreted from the cell (Rollins et al. 2000).

Flp-in, C-Src and N2-Src HeLa were co-transfected with the secretion reporter. On the same day, 5 h after the transient transfection, doxycycline was added to the medium to induce the expression of C-Src and N2-Src kinases. To verify that the secretion reporter construct was expressed by the cell lines and that its expression was equal between the cell lines, Flp-in, C-Src and N2-Src HeLa cell lines were transfected with the pc4s1-GFP-FM4-GH plasmid, and then treated with 25 μM rapamycin for 0, 60 and 120 min prior to lysis. The lysates were compared directly by Western blot for GFP, FLAG and actin (Fig. 17). The immunoblot revealed a single band for GFP of 79 kDa, likely representing the GFP-tagged cargo without growth hormone. Comparing the loading control (actin) with GFP, there was no significant difference in GFP intensity between cell lines or over the time course of rapamycin treatment. Moreover, the cell lines that were treated with doxycycline to induce the expression of c-Src and N2-Src kinase show a constant expression of the protein of interest during the time course. Unfortunately, Fig 17 has too high a background to do densitometry.

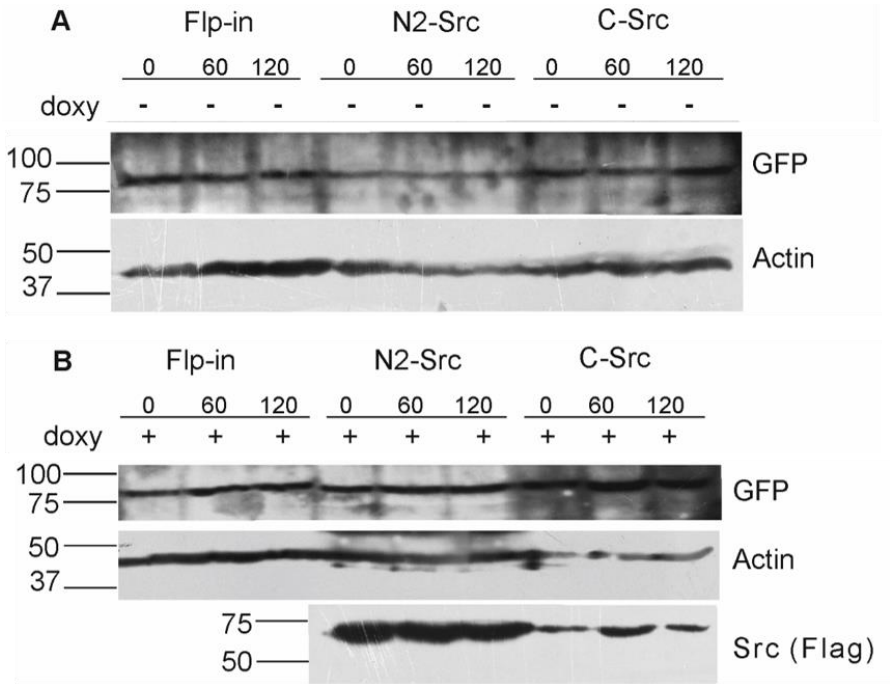

Figure 17. Expression of the pc4s1-GFP-FM4-GH plasmid in Flp-in HeLa (control), C-Src and N2-Src cell lines, with and without the addition of doxycycline. To verify the expression of the pc4s1-GFP-FM4-GH plasmid between the different cell lines with (B) or without (A) doxycycline, control, C-Src or N2-Src HeLa cells were transfected with the plasmid 24 h prior to the addition of 25 μL of rapamycin to induce secretion. The cells were then lysed in Laemmli buffer at 0 (control) 60 and 120 min after the addition of rapamycin was and analysed by immunoblotting for α-GFP, α-FLAG (Src) and α-actin.

Indeed, the eGFP tag in the secretion reporter construct permitted secretion to be visualized for changes in the vesicle distribution and quantified with optical-based approaches (Gordon et al. 2010). This was exploited to analyse changes in the distribution of vesicles during the expression of the kinases in analysis. The cell lines, with and without the addition of doxycycline to allow the expression of c-Src and N2-Src, were treated with 25 μl of rapamycin to induce secretion of the construct. It was observed that in the N2-Src expressing HeLa cells, N2-Src kinase induced a redistribution of the vesicles along neurite-like processes, which is most apparent 120 min after the addition of rapamycin, which allows the construct to be secreted. In contrast, in the other cell lines, the vesicles are located mostly close to the nucleus at all the time points analysed (Fig.18).

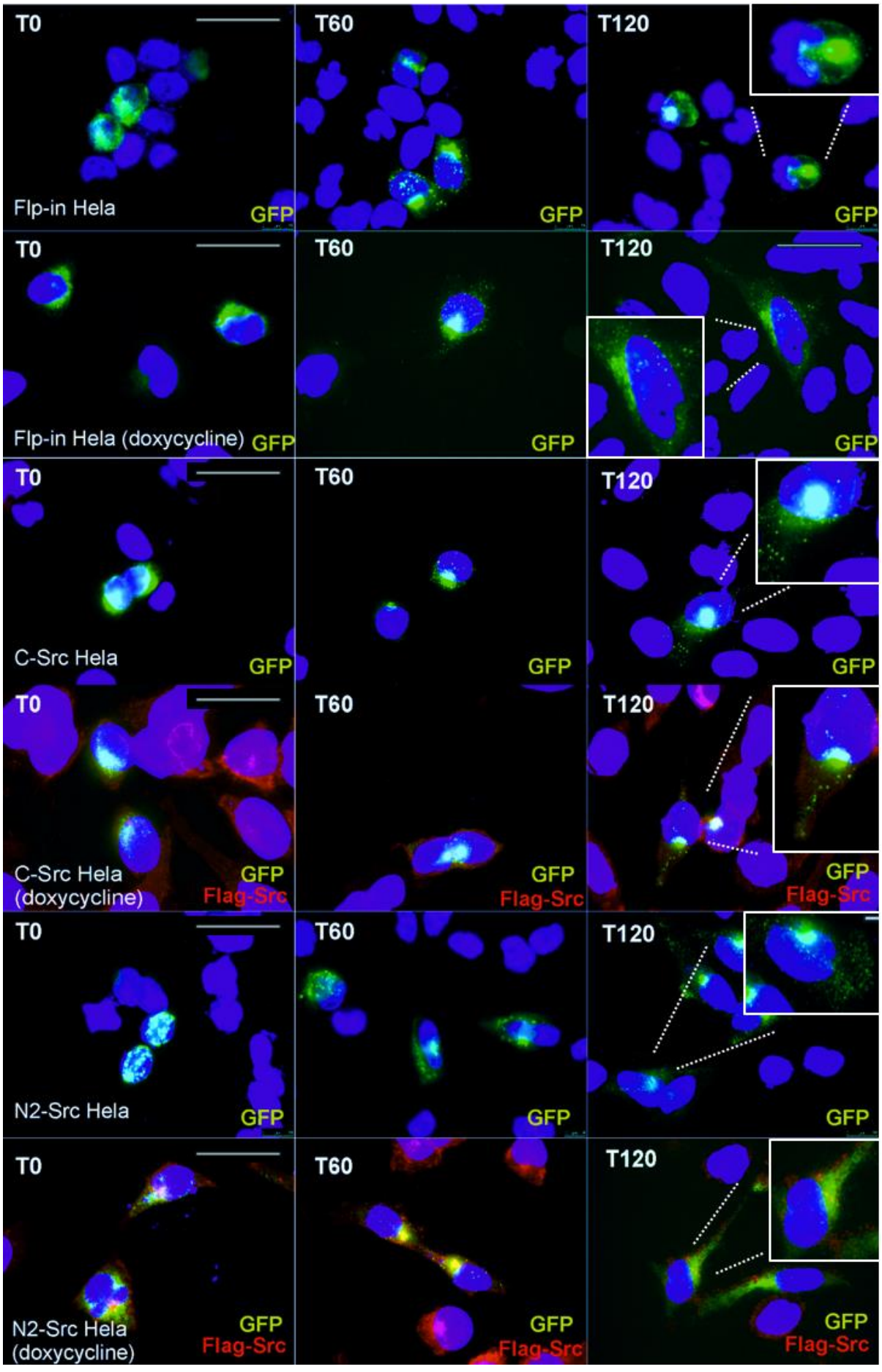
T0
T60
T120
Flp-in Hela
GFP
T0
T60
T120
Flp-in Hela (doxycycline)
GFP
T0
T60
T120
C-Src Hela
GFP
T0
T60
T120
C-Src Hela
(doxycycline)
GFP
Flag-Src
T0
T60
T120
N2-Src Hela
GFP
T0
T60
T120
N2-Src Hela
(doxycycline)
GFP
Flag-Src

Figure 18. Increased number and re-distribution of secretory vesicles along neurite-like processes in N2-Src kinase expressing HeLa cells. Flp-in (control), C-Src and N2-Src HeLa cell lines, with and without the addition of 1 µg/ml doxycycline were treated with rapamycin (1 µg/ml) and fixed at the indicated time points. Fixed cells were stained for Src (Flag; red), GFP (green) and DAPI (blue). Images were acquired with a wide-field fluorescent microscope. Scale bar = 50 µm. Insets show vesicles in a representative magnified area for each condition at the 120 min (T120) time point. In the N2-Src expressing HeLa cells, N2-Src kinase induced a redistribution of the vesicles along neurite-like processes, which is most apparent 120 min after the addition of rapamycin.

To better understand and quantify if N2-Src kinase is not only able to redistribute the vesicles along the neurite-like processes, but also to increase the average number of vesicles, 20 pictures per condition and time point were analysed using the "Squassh" segmentation method described in **2.7.2**. As can be seen in Fig.19A, the expression of N2-Src causes an increase in the mean number of vesicles per cell, which is particularly apparent at 120 min.

Since the increase in the mean number of vesicles per cell is greatest at 120 min for the cells that are expressing N2-Src, the distribution of vesicles per cell at this time point was presented with a dot and whisker plot (Fig. 19B). In Fig. 19B, not only the mean, which is a measure of central tendency and could be skewed by high values, but also the median confirmed the increase in the number of vesicles.

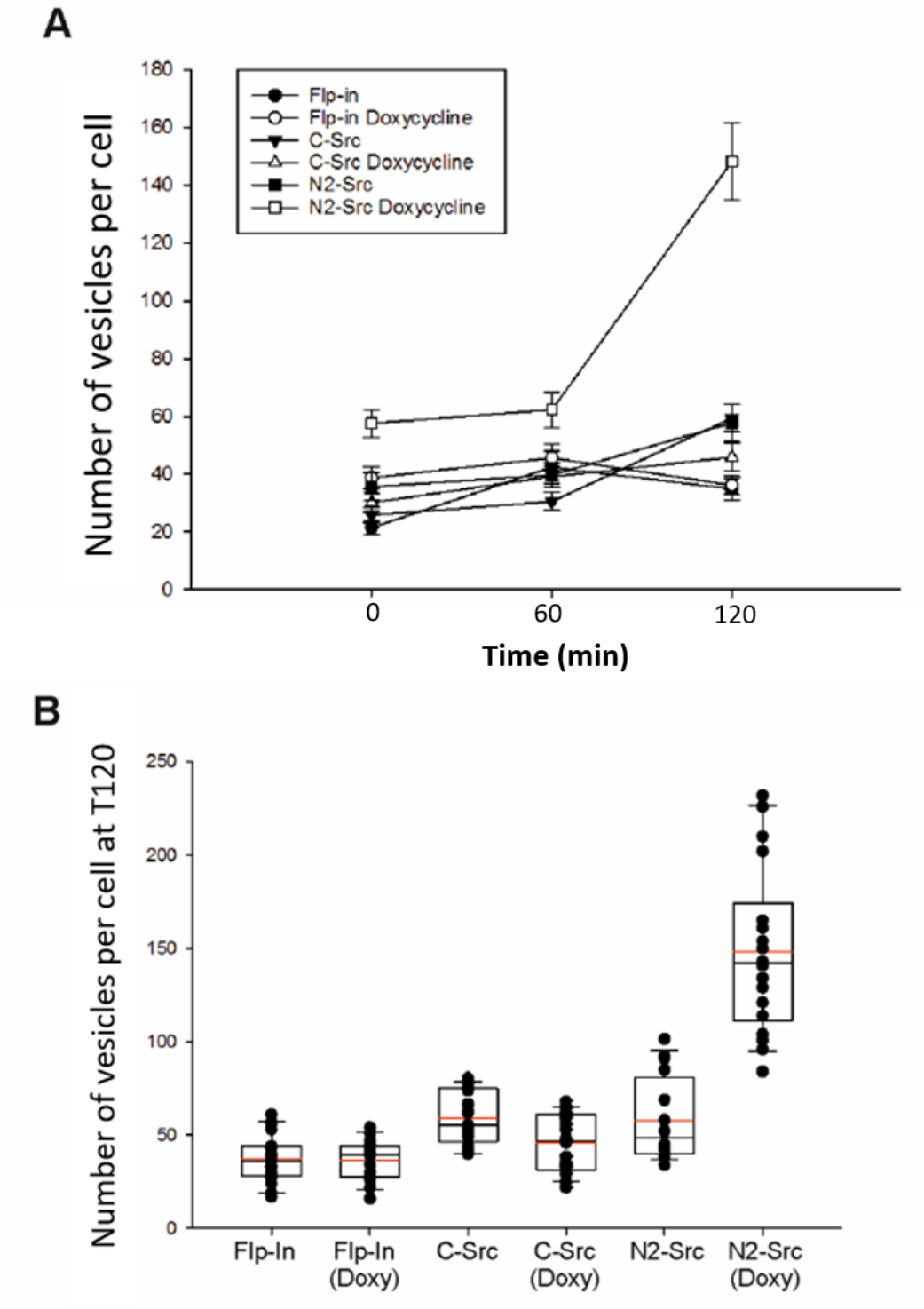

Figure 19. N2-Src causes an increase in the volume of COPII transport. The pictures of the different HeLa cell lines, with and without doxycycline and after the addition of rapamycin, were analysed through the "Squassh" segmentation method (described in **2.7.2**). (A) The number of vesicles per cell for each condition and at each time point was averaged; the average number of cells analysed for each condition is 20, from two independent experiments, and the data are plotted as mean number of vesicles per cell. (B) The vesicles distribution at T120 is depicted as a dot and whiskers plot, showing the median in black, the mean in red and the full range of the measurements.

3.5. Sec23A silencing

To develop reagents for investigating whether the effect of N2-Src on cell morphology and differentiation is mediated via Sec23A I validated four pSUPER constructs designed to silence the expression of Sec23A (Fig.20). It was decided to use plasmid-based delivery of short hairpin (sh) RNA because we have previously used this system to successfully knockdown protein expression in fibroblasts and neurons (Keenan et al., 2017). Furthermore, Korpal et al. (2011) were able to knockdown Sec23A using shRNAs to demonstrate it is a functional downstream target of miR-200 in metastasis. Complementary oligonucleotides encoding the shRNA sequences (see Material and Methods) and sticky ends for BglII and XhoI were annealed and ligated into pSUPER.mCherry/neo. The sticky ends were designed such that successful ligation would mutate the BglII site and thus clones were screened for a lack of BglII cleavage (Fig.20).

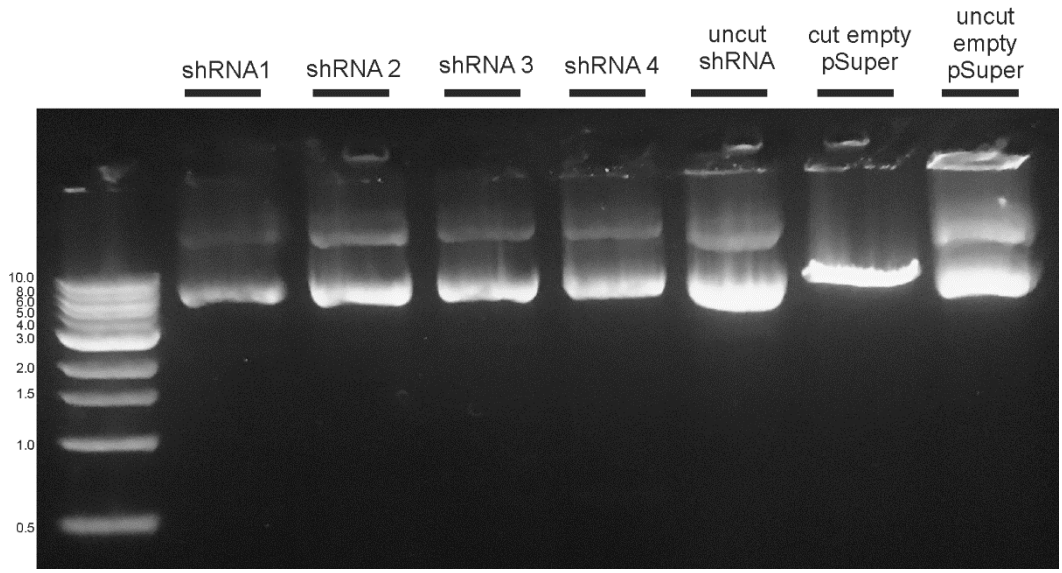

Figure 20. Screening for positive Sec23A-shRNA oligonucleotide ligation into pSUPER by BglII digestion. The purified plasmids digested with BglII are in the first four lanes while the last three lanes show control examples of an undigested shRNA plasmid, the empty plasmid vector digested with BglII and the undigested empty pSUPER plasmid.

To verify which Sec23A shRNAs were the most effective, two approaches were employed: i) attempted knockdown of endogenous Sec23A in HeLa cells and ii) knockdown of HA-Sec23A, over-expressed in HeLa cells (Fig.21). Firstly, Flp-in HeLa cells were transfected with the shRNAs alone and it was found that shRNAs 3 and 4 were able to decrease the endogenous expression of Sec23A (Fig.21A). Secondly, HeLa cells co-transfected with HA-

tagged Sec23A and the four pSUPER-Sec23A plasmids were assessed for HA immunoreactivity. Unfortunately, it was not possible to detect the expression of the HA-tagged Sec23A protein with an anti-HA antibody (data not shown), possibly due to a lack of sensitivity of the HA antibody, since bands were detected with an anti-Sec23A antibody.

In an attempt to detect the HA-tag of the transfected Sec23A, Flp-in HeLa cells were co-transfected with HA-tagged Sec23A and shRNA 3 and the cell lysates were subjected to an anti-HA immunoprecipitation. As can be seen in Figure 22B, it was possible to detect the presence of HA-Sec23A in the IP samples in both the lanes of HA-Sec23A+empty pSUPER and HA-Sec23A+scramble shRNA, while the expression of the protein was silenced in cells co-transfected with shRNA 3. Unfortunately, it was still not possible to detect the presence of the HA-tagged protein in the input, supporting the possibility that the HA antibody is not sensitive enough to detect exogenous HA-Sec23A unless enriched by immunoprecipitation. When the membrane was reprobed with the antibody against Sec23A, it was possible to detect the protein both in the IP and input samples and it was possible to confirm that the shRNA 3 is able to decrease the production of the Sec23A protein (Fig.21B). However, blotting with α-Sec23A should produce two bands, which represent the endogenous protein and HA-tagged one. The HA-tagged Sec23A should be heavier than the endogenous form, but it is possible the two bands run on top of each other.

Despite the promising results obtained, the knock down experiment should be repeated in order to confirm the silencing of Sec23A by the shRNA 3 and 4.

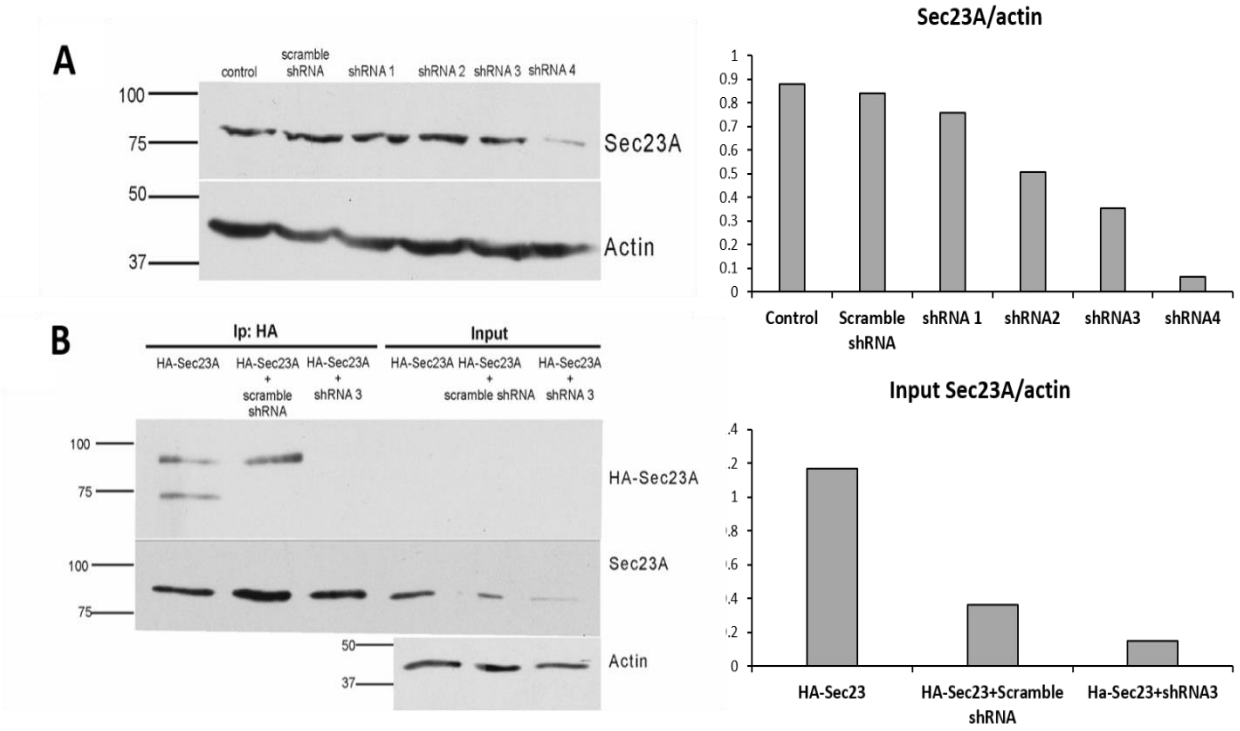

<u>Figure 21.</u> pSUPER-Sec23A shRNA knockdown of endogenous or overexpressed Sec23A in HeLa cells. (A) Flp-in HeLa cells were transfected with pSUPER shRNA (1-4) or non-targeting shRNA constructs for 48 h, then lysed in Laemmli buffer 2X and run on a SDS PAGE prior to immunoblotting with α-Sec23A and α-actin. ShRNA 3 and shRNA4 are able to decrease the endogenous expression of Sec23A, confirmed by the analysis of the relative intensities shown aside the Western Blot picture. (B) Flp-in HeLa cells were co-transfected with HA-Sec23A and pSUPER shRNA 3 or scramble shRNA for 48 h and then lysed. The lysates (inputs) were immunoprecipitated with an anti-HA antibody (IP:HA). Input and IP samples were separated by SDS PAGE and immunoblotted with α-HA, α-Sec23A or α-actin. Unfortunately, it was possible to detect the presence of the tagged HA-Sec23A only in the IP samples, possibly due to a loss of the HA-tag in the input samples. However, the presence of Sec23A was detected in both the IP and input samples once the membrane was reprobed with the α-Sec23A, where it was possible to notice a decrease in the Sec23A expression, as also confirmed by the analysis of the relative intensities shown aside the Western Blot picture.

4. Discussion

C-Src has two splice variants expressed solely in neuronal tissue (Brugge et al. 1985, Pyper and Bolen 1989), termed N1- and N2-Src. These two isoforms differ between each other only by 11 aminoacids: N1-Src arises from an insertion of the N1 mini-exon (six amino acids), while in N2-Src the N1 and N2 mini exons insert a total of seventeen amino acids. Although C-Src is found in all metazoans, N-Srcs have a more recent origin: N1-Src arises in low vertebrates (teleost fish; Raulf et al., 1989) and N2-Src only found in mammals.

Little is known about the functions of N1-Src, but it has often been linked with neuronal differentiation during development (Cartwright et al., 1988; Maness and Aubry, 1988; Kotani et al., 2007).

In contrast, the role of N2-Src tyrosine kinase in the development of the nervous system was first proposed through several clinical studies on neuroblastoma (Mellstrom et al. 1987, Bjelfman et al. 1990, Matsunaga et al. 1993, Hedborg et al. 1995, Matsunaga et al. 1998). In these studies, it was discovered that the high protein expression of N2-Src kinase positively correlates with the neuronal differentiation of neuroblastoma cell lines and a favourable outcome in neuroblastoma patients. Specifically, the N2 isoform is more common in infantile and localized neuroblastomas compared to metastatic disease (Matsunaga et al. 1998). Indeed, preliminary data from research performed in the Evans laboratory show that N2-Src kinase is able to induce the extension of neurite-like processes in neuroblastoma cell lines (SK-N-AS and Kelly), even those that are retinoic acid-resistant (Hernández Pérez 2015, Lewis 2014, Keenan et al. 2017). Moreover, the overexpression of this kinase, compared to the overexpression of C-Src or N1-Src kinase, produced the most significant effects on HeLa cell morphology and migration, thus confirming the previously speculated role of N2-Src in the acquisition of neuronal morphology (Lewis, 2014).

In this study, I have further investigated the relationship between N2-Src and the COPII complex in inducing the extension of neurite-like processes. By using a model cell line that inducibly expresses N2-Src kinase and through the analysis of morphological and migratory parameters, I was able to show an N2-Src trend in decreasing migration. I have also shown that N2-Src has a trend in influencing the rate of COPII transport. Moreover, the Sec23A silencing shRNAs that I have developed could be used to further investigate the molecular basis of this trend in relation to neuronal differentiation.

4.1. N2-Src reduces the cell track length

A previous study performed in my laboratory by Lewis (2014), showed that N2-Src is able to decrease cell proliferation in a wound healing assay. To gain further insights into migration in the N2-Src inducible cell line I used ptychography to quantify individual cell behaviour over time in culture.

Cell migration has an important role in many cellular processes, such as embryogenesis, immune surveillance and wound healing (Petrie, Doyle, and Yamada 2009) and it is possible to analyse two different types of migration: a random migration that occurs when a cell possesses low intrinsic directionality and explores its local environment (Jain, Worthylake, and Alahari 2012), and a directed migration, that may derive from external clues, such as chemoattractants, growth factors and extracellular matrix (Huttenlocher 2005). Src is involved in the modulation of many cellular processes and deregulation or altered expression is associated with human cancers (Acosta et al. 2003, Mayer and Krop 2010). In particular a role for Src in cell adhesion and motility was already found by Rohrschneider (1980) in fibroblasts transformed with the constitutively active v-Src that showed a round morphology and detachment from the extracellular matrix. Moreover, Src kinase promotes adhesion, migration and invasion through the direct binding of FAK, a tyrosine kinase (Baumgartner et al. 2008)

In this study, it was possible to give a further insight into the results obtained by Lewis (2014), despite the fact that the data obtained need more replicates to facilitate the statistical analysis : the decrease in the percentage area of the wound is higher for the C-Src Hela cell line treated with doxycycline compared to the N2-Src treated cells, particularly at the time point 24-48 h (Fig. 13A). It was also possible to analyse the single cell behaviour and evaluate the track length of each cell, thus confirming the trend of the C-Src cells expressing the kinase that have a higher median track length, which is indicative of a more explorative behaviour (Fig. 13B). Interestingly, C-Src cells not treated with doxycycline showed a higher percentage decrease of the wound area in the first 24 h analysed, but the same median track length as N2-Src Hela cells not treated: this could be seen as an higher mitotic behaviour of the C-Src cells that try to fill the scratched area, noticeable also from the examination of the time-lapse pictures.

Regarding the random migration assay, the analysis of the time lapse images revealed that the C-Src HeLa cells explored their environment more, as evidenced by an increase in the single cell track length, compared with N2-Src HeLa cells (Fig. 15A). Moreover, a higher number of N2-Src cells did not move at all, compared to the C-Src cells (Fig. 15B). A visual examination of the time-lapse picture frames showed an interesting trend that needs to be confirmed by more biological replicates: the decrease in the number of cells undergoing mitosis between C-Src and N2-Src. While the C-Src cells where frequently dividing successfully, the N2-Src cells seemed to attempt dividing by rounding up, but then failing and starting to protrude neurite-like processes. Unfortunately, the CAT analysis software was unable to quantify the mitotic index of the cells, but this feature should be implemented in the future, in order to be able to properly detect and quantify cells that round up.

During cell adhesion and motility, a role for Src was already indicated by Rohrschneider (1980), who observed that transformation with the constitutively active v-Src causes a round morphology and detachment from the ECM. In the migration context, a fundamental role is played by cell surface receptors and components of the extracellular matrix: in particular, integrin receptor binding initiates signals that stimulate tyrosine phosphorylation of intracellular proteins including members of the Src family and the focal adhesion kinase (FAK), providing a link between the extracellular matrix proteins and components of the intracellular space (Carey 1991, Gumbiner 1996, Short, Talbott, and Juliano 1998, Sieg et al. 2000). Notably, it has been shown that during cell adhesion, members of the Src family kinases translocate to focal adhesions and regulate rearrangement of actin structures: for example, the overexpression of an inactive form of Src reduces the rate of vascular smooth muscle cell spreading on collagen, while the wild-type form of this kinase enhances spreading (Ishida et al. 1999). These observations strengthen the idea that Src kinase activity is required for cytoskeletal reorganization and signal transduction at the focal adhesion during migration, even if the full activation of Src kinase is achieved only through the association with FAK, in a sort of synergism that eventually promote cell migration (Carragher et al. 2003, Hsia et al. 2003).

It would be then useful to explore more deeply the role of Src kinase during motility and migration. In particular, it would be interesting understanding the exact role and regulation of N2-Src during this cellular process by taking advantage of the live cell imaging and these

two assays, considering the many interactions that are known to happen between Src and other intracellular components. One possibility would be combining the live cell imagining with fluorescent shRNA to knockdown the expression of some protein of interest that may be related to this process. More specifically, in order to gain better insights on the interplay between Src and the COPII transport during migration, one of the first experiments in this direction may profit from the shRNA I developed and tested in this study, to knock down the expression of Sec23A and verify differences in cell migration and proliferation.

4.2. N2-Src redistributes and increases the number of available secretory vesicles

I have studied the effect of N2-Src upon COPII transport by observing vesicular structures following release of a fluorescent cargo from the ER in the HeLa cell line that inducibly expresses N2-Src kinase. In my experiments, I observed the trend of a redistribution of the vesicles along the neurite-like processes that the cells expressing N2-Src kinase possess, which could be due to the demand for new membrane to extend these formations (Fig. 18). To gain a deeper insight into the trend of N2-Src dependent changes in vesicle distribution, the number of vesicles for each cell line and at each time point was quantified in two biological replicates and it was observed that N2-Src increases the number of vesicles, most noticeable 2 h after cargo release (Fig. 19), when more than 80% of the cargo in the pc4s1-GFP-FM4-GH plasmid has been secreted (Rollins et al. 2000).

Neuronal differentiation is a process that requires the establishment of polarity in the cell, defined by the oriented extension of axons and dendrites (Bauch, Stier, and Schlosshauer 1998). Neurons can protrude a long extended axon and elaborate dendritic arbours (Horton and Ehlers 2003) that can produce a surface area 10,000 times greater than typical cells, producing structures hundreds of microns away from the cell body (Horton and Ehlers 2004). The outgrowth of processes is therefore a crucial event during the development of the nervous system that involves coordinated and widespread regulation of the cytoskeleton and the membrane trafficking machinery (Foletti, Prekeris, and Scheller 1999, da Silva and Dotti 2002), but it also requires a large addition of plasma membrane (Gauthier et al. 2009, Prager-Khoutorsky and Spira 2009). Indeed, the principal sites of synthesis of lipid, integral membrane proteins and growth factors needed to support localized signalling are the

organelles of the secretory pathway, in particular the ER and Golgi apparatus (Horton et al. 2005). Therefore, in order to establish a polarity, the new membrane produced through the secretory pathway is added to the apical side of the cells early in polarization during neurite growth in development and differentiation (Tang 2008), also through the exocytosis process, that is balanced by the internalization of membrane through endocytosis (Ye et al. 2007).

It has been demonstrated that targeted secretory trafficking controls the growth of plasma membrane in several processes in many different cell types, for example in yeast cell during budding, or more in general during cell migration (Bergmann, Kupfer, and Singer 1983, Etienne-Manneville and Hall 2003, Kupfer, Dennert, and Singer 1983). In this study, the increase in the number of vesicles seen in the HeLa cells that were expressing N2-Src kinase is possibly due to the neurite-like processes outgrowth, a mechanism that requires the addition of plasma membrane, which is also provided by the process of exocytosis. The spatial control over the organization of secretory trafficking may provide a general mechanism for the formation of elaborate processes like dendrites and axons (Horton et al. 2005), therefore it has also been shown in neurons that the secretory pathway has a unique spatial distribution (Gardiol, Racca, and Triller 1999, Horton and Ehlers 2003, Pierce, Mayer, and McCarthy 2001): the neuronal Golgi is composed of both Golgi stacks in the cell body and discrete Golgi outposts in dendrites that can be synapse-associated (Gardiol, Racca, and Triller 1999, Pierce, Mayer, and McCarthy 2001); *trans* Golgi network (TGN) organelles in dendrites localize at sites of neuron-neuron contact (Sytnyk et al. 2002).

It has been also proven that during dendritic outgrowth there is an increase in the number of dendritic ER exit sites (ERES), where secretory cargoes bud from the ER directed to the Golgi (Aridor et al. 2001). Consequently, the organization of the secretory trafficking during neuronal differentiation relies not only on the spatial distribution, but also on the increase of the vesicles budding sites. Indeed, in a previous study in the Evans laboratory (Hernández Pérez 2015), it was shown that the protein expression of N2-Src causes redistribution of ERES, spreading in a larger perinuclear region that is not restricted anymore to the ER-Golgi intermediate compartment (ERGIC) region (Fig.22). This ERES redistribution could possibly be an explanation of the trend seen in my study, in which N2-Src expressing cells show a redistribution of the vesicles along the outgrowing neurite-like processes.

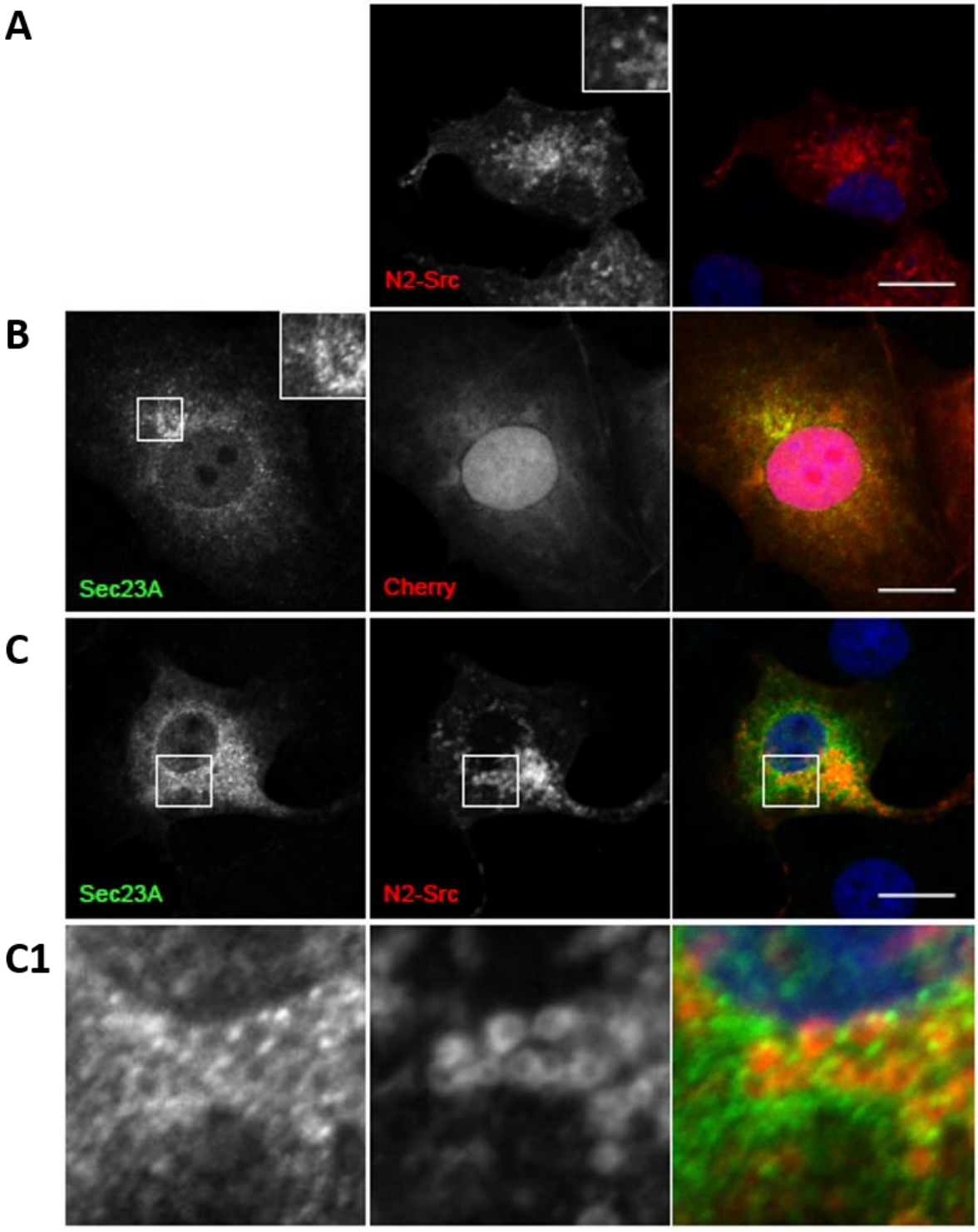

Figure 22. N2-Src induces ERES dispersion in the perinuclear region. Co-expressed N2-Src and Sec23A did not colocalise, despite being in the same area. Interestingly, N2-Src overexpression caused a redistribution of ERES which is no longer restricted to ERGIC-like staining but distributed in a larger perinuclear region, which matches with the region to which N2-Src is localised. (A-C) COS7 cells were transfected with a HA-Sec23A or a control plasmid and with an N2-Src-Cherry or a control plasmid. The scale bar represents 20 µm. (C1) Magnified pictures of the indicated sections in C (modified from Hernández Pérez 2015).

Therefore, it is possible to hypothesize that this N2-Src trend seen in my study may be due to the larger number of ERES available for the vesicles to bud, but also for the wider area available for the ERES distribution (Fig.23). However, this interesting trend that emerges in my experiments needs to be confirmed by more biological replicates to facilitate the statistical analysis of the data.

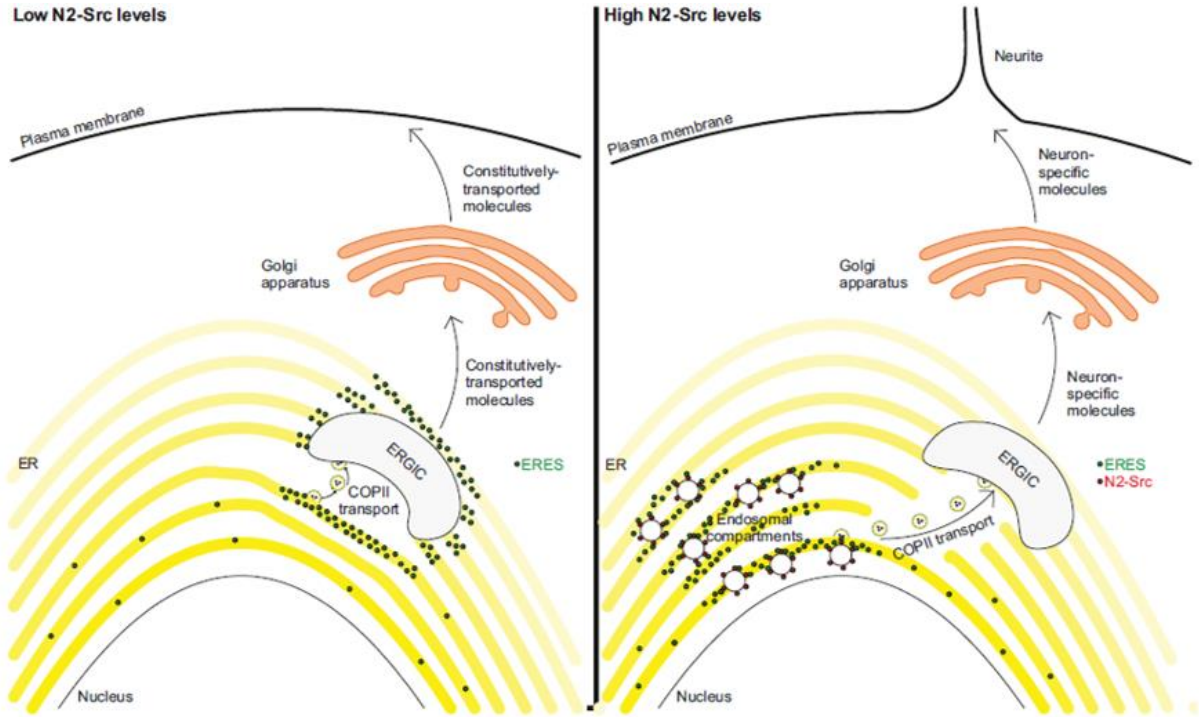

Figure 23. Possible model for N2-Src induced increase of the number of vesicles in N2-Src expressing HeLa cells. Under low N2-Src levels, COPII vesicles are formed at ERES and transported to the ERGIC, from where cargoes continue their delivery to other organelles. When there is a high expression of N2-Src, ERES are increased and redistributed around endosomal compartments and become accessible to N2-Src. N2-Src binds and phosphorylates COPII components, modifying vesicle formation. As a consequence, the increase seen in the number of vesicles might be due to the increase in the number of ERES available, but also for the wider area available for the ERES distribution (modified from Hernández Pérez 2015).

However, given the fundamental role of the secretory trafficking in many aspects of neuronal function, like synapse formation, synaptic plasticity, but in particular neuronal differentiation (Bradke and Dotti 2000, Craig, Wyborski, and Banker 1995, Song and Poo 1999), it will be important for future studies to verify this increase seen in this biological model in a RA-resistant neuroblastoma cell line. Furthermore, it has been already seen and demonstrated that phosphorylation of the COPII complex components may activate COPII and re-direct it to different pathways. An example of this could be the work of Wang et al. 2015 and Davis et al. 2016, in which they demonstrated how the phosphorylation of Sec24, a

component of the COPII inner coat, by the casein kinase 1 (CK1), Hrr25, contributes to regulate autophagosome abundance during nutrient deprivation. It will be therefore fundamental to delineate exactly which member of the COPII complex is phosphorylated by N2-Src and how this phosphorylation determines the increase in the number of vesicles seen in this study.

4.3. Sec23A putative role in N2-Src neuroblastoma differentiation

Another finding in the previous study by Hernández Pérez (2015) was the putative involvement of Sec23A, protein member of the COPII complex, in N2-Src induced neurite outgrowth through the increase in the percentage of cells with processes and in the number of processes per cell in both COS7 and SK-N-AS cells. The data were preliminary and the number of SK-N-AS cells that presented neurites was too small for statistical analysis, but neurite outgrowth in cells that overexpressed Sec23A in addition to N2-Src was abolished when compared to N2-Src only overexpressing cells. If this finding is verified, it would strengthen the idea of the involvement of COPII transport in neuronal differentiation, in particular through the possible interplay between N2-Src and Sec23A.

In this study, I designed and validated some shRNA constructs able to silence the expression of Sec23A, which can then be used to test the aforementioned hypothesis.

The validation experiments were performed in HeLa cells and it was relevant to evaluate the efficacy of the shRNAs in silencing the endogenous expression of Sec23A (Fig. 22A). Afterwards, in order to further expand the data obtained with the silencing of the endogenous expression, I co-transfected the cells with the shRNA 3 for Sec23A and an HA-tagged Sec23A plasmid in order to overexpress the protein. Unfortunately, it was possible to detect the HA-tag only in the IP samples and not in the input ones (Fig. 22B). This result could be explained by a sensitivity issue or the loss of the HA-tag altogether, since, when the membrane was reprobed for Sec23A, it was possible to detect Sec23A and also to notice a decrease in the protein expression for some shRNAs (Fig. 21B).

I was not able to perform experiments in NB cells, but these tools I validated could be used to silence the expression of Sec23A and determine its role in neuroblastoma differentiation, and in general in cancer, since so far the role of this protein has been

controversial. For example, work by Szczyrba et al. (2011) demonstrated that the overexpression of Sec23A reduces cell growth and proliferation in carcinoma cells, but also a work by Korpal et al. (2011) showed that the inhibition of Sec23A prevents the secretion of metastasis-suppressive proteins, inhibiting migration but increasing colonization.

In neuroblastoma differentiation, it has been hypothesized that N2-Src could phosphorylate Sec23A, which is partially responsible, together with Sec24, for the selection of the cargo proteins to incorporate into secretory vesicles. The N2-Src phosphorylation could alter vesicle formation and it could also regulate the cargo specificity through Sec23A. Consequently, N2-Src may increase the transport of membrane proteins and lipids to promote neurite outgrowth or other processes necessary for neuronal differentiation.

Therefore, complementary experiments silencing Sec23A should be performed in order to discriminate between a positive or negative effect of the protein in neuroblastoma, and more specific, in N2-Src induced neuronal differentiation. The development and validation of some shRNAs is then very useful to help understanding the molecular mechanisms of the secretory pathway regulation in the context of neuroblastoma and, in general, neuronal differentiation, which is still largely unknown.

4.4. New insights for neuroblastoma differentiation therapies

My work on the fundamental effect of N2-Src on COPII transport was undertaken with the aim of better understanding neuroblastoma differentiation. So far, the long-term survival for high-risk neuroblastoma patients with current treatments is approximately 54% (Maris 2010). Unfortunately, patients with aggressively treated, high-risk neuroblastoma may develop late recurrences, some more than 5 years after completion of therapy (Mertens et al. 2001, Cotterill, Parker, et al. 2001, Cotterill, Pearson, et al. 2001) and the overall EFS and OS for stage 4 and 4S disease and MYCN-amplification was only 30% at 2 to 5 years after treatment in a European study (Canete et al. 2009).

Despite the use of isotretinoin (also known as 13-cis-retinoic acid) as a maintenance treatment for high-risk neuroblastoma cases has been shown to improve the EFS, only 10 to 20% of patients benefit from this differentiation therapy (PDQ 2017, Reynolds 2004) and the neuroblastoma cells left after initial chemotherapy treatments are highly resistant. For this reason, there is the need for more efficient and less toxic differentiation therapies.

One of the possible therapeutic strategies which is able to induce differentiation and senescence in specific neuroblastoma cell lines (Clark, Daga, and Stoker 2013) involves the use of oxovanadium compounds (Clark et al. 2015). These compounds are inhibitors of protein tyrosine phosphatases (PTPs) (Huyer et al. 1997), the key positive and negative modulators of ALK and MYCN action through AKT phosphotyrosine signalling (Qiao et al. 2013).

Another possible promising strategy would be to increase the expression of N2-Src kinase in the tumour cells, which unfortunately is not a simple therapeutic approach, even if it could induce differentiation.

A new interesting, and maybe more feasible, therapeutic target would be the silencing of the protein Sec23A by using an shRNA: if the silencing of Sec23A, member of the COPII, determines an increase in neuronal differentiation both in a model system (like the HeLa cells used in this study), but also in RA-resistant neuroblastoma cell lines (like the SK-N-AS cells), the construct could be delivered to the remaining tumour cell after the surgery, together with the RA in order to induce differentiation. Identification of tumour antigens is a growing field, due to the expanding field of immunotherapeutic treatments, and new antigens are found very frequently. For example, one of the antigens that could be useful to deliver Sec23A shRNA may be PRAME: PRAME (preferentially expressed antigen in melanoma), a cancer-testis antigen (CTA) that was first discovered in a patient with melanoma (Ikeda et al. 1997), but later found to be expressed in a large variety of cancer cells. A study by (Oberthuer et al. 2004) found that PRAME is universally expressed by high-risk neuroblastoma tumours, which are usually associated with poor outcome, therefore the possibility to use the Sec23A shRNA in order to differentiate the left tumour cells may be beneficial to the patients. However, a deeper understanding of the role of the COPII complex, and in particular Sec23A, during neuroblastoma differentiation could help in finding more efficient therapies to treat neuroblastoma patients.

Definitions and abbreviations

ALK	Anaplastic lymphoma receptor tyrosine kinase
bHLHZip	Basic-region/helix-loop-helix/leucine-zipper
BMP	Bone morphogenetic protein
BSA	Bovine serum albumin
CAT	Cell Analysis Toolbox
CDI	Coherent diffractive imaging
CLSD	Cranio–lenticulo–sutural dysplasia
COPII	Coat protein complex II
CrebA	cAMP response element-binding protein
CTA	Cancer-testis antigen
DAPI	4,6-Diamidino-2-phenylindole
DMEM	Dulbecco's modified Eagle's medium
DNA	Deoxyribonucleic Acid
EDTA	Ethylenediaminetetraacetic acid
EFS	Event free survival
EGTA	Ethyleneglycoltetraacetic acid
ER	Endoplasmatic reticulum
ERES	ER exit sites
ERGIC	ER-Golgi intermediate compartment
FAK	Focal adhesion kinase
FCS	Foetal calf serum
GO	Gene Ontology
GDP	Guanosine 5'-Diphosphate
GFP	Green fluorescent protein
GH	Growth hormone

GTP	Guanosine-5'-triphosphate
GTPase	Guanosinetriphosphatase
HRP	Horseradish peroxidase
INSS	International Neuroblastoma Staging System
IP	Immunoprecipitation
LB	Lysogeny broth
LTP	Long term potentiation
MYCN	V-Myc avian myelocytomatosis viral oncogene neuroblastoma derived homolog
MOPS	3-(N-morpholino)propanesulfonic acid
MS/MS	Tandem mass spectrometry
NGF	Neural growth factor
NMDA	N-Methyl-D-aspartate
OS	Overall survival
PBS	Phosphate-buffered saline
PEI	Polyethylenimine
Pen/strep	Penicillin/streptomycin
PRAME	Preferentially expressed antigen in melanoma
PSF	Point spread function
PVDF	Polyvinylidene difluoride
RA	Retinoic acid
RAREs	RA response elements
RARs	RA receptors
RXR	Retinoid X receptor
RNA	Ribonucleic acid
ROI	Region of interest

RSV	Rous sarcoma virus
SDS-PAGE	Sodium dodecyl sulfate-polyacrylamide gel electrophoresis
SFK	Src family kinases
SH	Src homology domain
shRNA	Short hairpin RNA
STRING	Search Tool for the Retrieval of Interacting Genes/Proteins
SV	Synaptic vesicles
TAE	Tris base, acetic acid and EDTA
TEMED	Tetramethylethylenediamine
TGN	*Trans* Golgi network
Tris	Tris(hydroxymethyl)aminomethane

List of references

Acosta, J. J., R. M. Munoz, L. Gonzalez, A. Subtil-Rodriguez, M. A. Dominguez-Caceres, J. M. Garcia-Martinez, A. Calcabrini, I. Lazaro-Trueba, and J. Martin-Perez. 2003. "Src mediates prolactin-dependent proliferation of T47D and MCF7 cells via the activation of focal adhesion kinase/Erk1/2 and phosphatidylinositol 3-kinase pathways." *Mol Endocrinol* 17 (11):2268-82.

Acosta, S., C. Lavarino, R. Paris, I. Garcia, C. de Torres, E. Rodriguez, H. Beleta, and J. Mora. 2009. "Comprehensive characterization of neuroblastoma cell line subtypes reveals bilineage potential similar to neural crest stem cells." *BMC Dev Biol* 9:12.

Antonny, B., D. Madden, S. Hamamoto, L. Orci, and R. Schekman. 2001. "Dynamics of the COPII coat with GTP and stable analogues." *Nat Cell Biol* 3 (6):531-7.

Aridor, M., and K. N. Fish. 2009. "Selective targeting of ER exit sites supports axon development." *Traffic* 10 (11):1669-84.

Aridor, M., K. N. Fish, S. Bannykh, J. Weissman, T. H. Roberts, J. Lippincott-Schwartz, and W. E. Balch. 2001. "The Sar1 GTPase coordinates biosynthetic cargo selection with endoplasmic reticulum export site assembly." *J Cell Biol* 152 (1):213-29.

Aridor, M., A. K. Guzik, A. Bielli, and K. N. Fish. 2004. "Endoplasmic reticulum export site formation and function in dendrites." *J Neurosci* 24 (15):3770-6.

Aridor, M., J. Weissman, S. Bannykh, C. Nuoffer, and W. E. Balch. 1998. "Cargo selection by the COPII budding machinery during export from the ER." *J Cell Biol* 141 (1):61-70.

Arimura, N., and K. Kaibuchi. 2007. "Neuronal polarity: from extracellular signals to intracellular mechanisms." *Nat Rev Neurosci* 8 (3):194-205.

Ascione, F., A. Vasaturo, S. Caserta, V. D'Esposito, P. Formisano, and S. Guido. 2016. "Comparison between fibroblast wound healing and cell random migration assays in vitro." *Exp Cell Res* 347 (1):123-32.

Baldelli, P., A. Fassio, F. Valtorta, and F. Benfenati. 2007. "Lack of synapsin I reduces the readily releasable pool of synaptic vesicles at central inhibitory synapses." *J Neurosci* 27 (49):13520-31.

Barlowe, C., C. d'Enfert, and R. Schekman. 1993. "Purification and characterization of SAR1p, a small GTP-binding protein required for transport vesicle formation from the endoplasmic reticulum." *J Biol Chem* 268 (2):873-9.

Barlowe, C., L. Orci, T. Yeung, M. Hosobuchi, S. Hamamoto, N. Salama, M. F. Rexach, M. Ravazzola, M. Amherdt, and R. Schekman. 1994. "COPII: a membrane coat formed by Sec proteins that drive vesicle budding from the endoplasmic reticulum." *Cell* 77 (6):895-907.

Bauch, H., H. Stier, and B. Schlosshauer. 1998. "Axonal versus dendritic outgrowth is differentially affected by radial glia in discrete layers of the retina." *J Neurosci* 18 (5):1774-85.

Baumgartner, Martin, Gerald Radziwill, Mihaela Lorger, Andreas Weiss, and Karin Moelling. 2008. "c-Src-Mediated Epithelial Cell Migration and Invasion Regulated by PDZ Binding Site."

Beckwith, J. B., and E. V. Perrin. 1963. "In Situ Neuroblastomas: A Contribution to the Natural History of Neural Crest Tumors." *Am J Pathol* 43:1089-104.

Bergmann, J. E., A. Kupfer, and S. J. Singer. 1983. "Membrane insertion at the leading edge of motile fibroblasts." *Proc Natl Acad Sci U S A* 80 (5):1367-71.

Bi, X., R. A. Corpina, and J. Goldberg. 2002. "Structure of the Sec23/24-Sar1 pre-budding complex of the COPII vesicle coat." *Nature* 419 (6904):271-7.

Bi, X., J. D. Mancias, and J. Goldberg. 2007. "Insights into COPII coat nucleation from the structure of Sec23.Sar1 complexed with the active fragment of Sec31." *Dev Cell* 13 (5):635-45.

Binz, K. 2016. "kevinbinz.com."

Bjelfman, C., F. Hedborg, I. Johansson, M. Nordenskjold, and S. Pahlman. 1990. "Expression of the neuronal form of pp60c-src in neuroblastoma in relation to clinical stage and prognosis." *Cancer Res* 50 (21):6908-14.

Bjorge, J. D., A. Jakymiw, and D. J. Fujita. 2000. "Selected glimpses into the activation and function of Src kinase." *Oncogene* 19 (49):5620-35.

Boussif, O., F. Lezoualc'h, M. A. Zanta, M. D. Mergny, D. Scherman, B. Demeneix, and J. P. Behr. 1995. "A versatile vector for gene and oligonucleotide transfer into cells in culture and in vivo: polyethylenimine." *Proc Natl Acad Sci U S A* 92 (16):7297-301.

Bradke, F., and C. G. Dotti. 2000. "Establishment of neuronal polarity: lessons from cultured hippocampal neurons." *Curr Opin Neurobiol* 10 (5):574-81.

Briggs, S. D., and T. E. Smithgall. 1999. "SH2-kinase linker mutations release Hck tyrosine kinase and transforming activities in Rat-2 fibroblasts." *J Biol Chem* 274 (37):26579-83.

Brodeur, G. M., J. Pritchard, F. Berthold, N. L. Carlsen, V. Castel, R. P. Castelberry, B. De Bernardi, A. E. Evans, M. Favrot, F. Hedborg, and et al. 1993. "Revisions of the international criteria for neuroblastoma diagnosis, staging, and response to treatment." *J Clin Oncol* 11 (8):1466-77.

Bronner, M. E., and N. M. LeDouarin. 2012. "Development and evolution of the neural crest: an overview." *Dev Biol* 366 (1):2-9.

Brown, M. T., and J. A. Cooper. 1996. "Regulation, substrates and functions of src." *Biochim Biophys Acta* 1287 (2-3):121-49.

Brugge, J. S., P. C. Cotton, A. E. Queral, J. N. Barrett, D. Nonner, and R. W. Keane. 1985. "Neurones express high levels of a structurally modified, activated form of pp60c-src." *Nature* 316 (6028):554-7.

Burgo, A., A. M. Casano, A. Kuster, S. T. Arold, G. Wang, S. Nola, A. Verraes, F. Dingli, D. Loew, and T. Galli. 2013. "Increased activity of the vesicular soluble N-ethylmaleimide-sensitive factor attachment protein receptor TI-VAMP/VAMP7 by tyrosine phosphorylation in the Longin domain." *J Biol Chem* 288 (17):11960-72.

Bushue, N., and Y. J. Wan. 2010. "Retinoid pathway and cancer therapeutics." *Adv Drug Deliv Rev* 62 (13):1285-98.

Canete, A., M. Gerrard, H. Rubie, V. Castel, A. Di Cataldo, C. Munzer, R. Ladenstein, B. Brichard, J. D. Bermudez, J. Couturier, B. de Bernardi, A. J. Pearson, and J. Michon. 2009. "Poor survival for infants with MYCN-amplified metastatic neuroblastoma despite intensified treatment: the International Society of Paediatric Oncology European Neuroblastoma Experience." *J Clin Oncol* 27 (7):1014-9.

Carey, D. J. 1991. "Control of growth and differentiation of vascular cells by extracellular matrix proteins." *Annu Rev Physiol* 53:161-77.

Carragher, N. O., M. A. Westhoff, V. J. Fincham, M. D. Schaller, and M. C. Frame. 2003. "A novel role for FAK as a protease-targeting adaptor protein: regulation by p42 ERK and Src." *Curr Biol* 13 (16):1442-50.

Chen, Y., J. Takita, Y. L. Choi, M. Kato, M. Ohira, M. Sanada, L. Wang, M. Soda, A. Kikuchi, T. Igarashi, A. Nakagawara, Y. Hayashi, H. Mano, and S. Ogawa. 2008. "Oncogenic mutations of ALK kinase in neuroblastoma." *Nature* 455 (7215):971-4.

Cheng, M., and G. R. Ott. 2010. "Anaplastic lymphoma kinase as a therapeutic target in anaplastic large cell lymphoma, non-small cell lung cancer and neuroblastoma." *Anticancer Agents Med Chem* 10 (3):236-49.

Chong, Y. P., T. D. Mulhern, H. J. Zhu, D. J. Fujita, J. D. Bjorge, J. P. Tantiongco, N. Sotirellis, D. S. Lio, G. Scholz, and H. C. Cheng. 2004. "A novel non-catalytic mechanism employed by the C-terminal Src-homologous kinase to inhibit Src-family kinase activity." *J Biol Chem* 279 (20):20752-66.

Clark, O., S. Daga, and A. W. Stoker. 2013. "Tyrosine phosphatase inhibitors combined with retinoic acid can enhance differentiation of neuroblastoma cells and trigger ERK- and AKT-dependent, p53-independent senescence." *Cancer Lett* 328 (1):44-54.

Clark, O., I. Park, A. Di Florio, A. C. Cichon, S. Rustin, R. Jugov, R. Maeshima, and A. W. Stoker. 2015. "Oxovanadium-based inhibitors can drive redox-sensitive cytotoxicity in neuroblastoma cells and synergise strongly with buthionine sulfoximine." *Cancer Lett* 357 (1):316-27.

Cohn, S. L., A. D. Pearson, W. B. London, T. Monclair, P. F. Ambros, G. M. Brodeur, A. Faldum, B. Hero, T. Iehara, D. Machin, V. Mosseri, T. Simon, A. Garaventa, V. Castel, and K. K. Matthay. 2009. "The International Neuroblastoma Risk Group (INRG) classification system: an INRG Task Force report." *J Clin Oncol* 27 (2):289-97.

Collett, J. W., and R. E. Steele. 1992. "Identification and developmental expression of Src+ mRNAs in Xenopus laevis." *Dev Biol* 152 (1):194-8.

Collett, M. S., E. Erikson, A. F. Purchio, J. S. Brugge, and R. L. Erikson. 1979. "A normal cell protein similar in structure and function to the avian sarcoma virus transforming gene product." *Proc Natl Acad Sci U S A* 76 (7):3159-63.

Cotterill, S. J., L. Parker, L. More, and A. W. Craft. 2001. "Neuroblastoma: changing incidence and survival in young people aged 0-24 years. A report from the North of England Young Persons' Malignant Disease Registry." *Med Pediatr Oncol* 36 (1):231-4.

Cotterill, S. J., A. D. Pearson, J. Pritchard, J. A. Kohler, A. B. Foot, Group European Neuroblastoma Study, and Group United Kingdom Children's Cancer Study. 2001. "Late relapse and prognosis for neuroblastoma patients surviving 5 years or more: a report from the European Neuroblastoma Study Group "Survey"." *Med Pediatr Oncol* 36 (1):235-8.

Craig, A. M., R. J. Wyborski, and G. Banker. 1995. "Preferential addition of newly synthesized membrane protein at axonal growth cones." *Nature* 375 (6532):592-4.

Cunningham, T. J., and G. Duester. 2015. "Mechanisms of retinoic acid signalling and its roles in organ and limb development." *Nat Rev Mol Cell Biol* 16 (2):110-23.

D'Arcangelo, J. G., K. R. Stahmer, and E. A. Miller. 2013. "Vesicle-mediated export from the ER: COPII coat function and regulation." *Biochim Biophys Acta* 1833 (11):2464-72.

da Silva, J. S., and C. G. Dotti. 2002. "Breaking the neuronal sphere: regulation of the actin cytoskeleton in neuritogenesis." *Nat Rev Neurosci* 3 (9):694-704.

Darnell, D., and S. F. Gilbert. 2017. "Neuroembryology." *Wiley Interdiscip Rev Dev Biol* 6 (1).

Davis, Saralin, Juan Wang, Ming Zhu, Kyle Stahmer, Ramya Lakshminarayan, Majid Ghassemian, Yu Jiang, Elizabeth A Miller, and Susan Ferro-Novick. 2016. "Sec24 phosphorylation regulates autophagosome abundance during nutrient deprivation."

De Bernardi, B., V. Mosseri, H. Rubie, V. Castel, A. Foot, R. Ladenstein, G. Laureys, M. Beck-Popovic, A. F. de Lacerda, A. D. Pearson, J. De Kraker, P. F. Ambros, Y. de Rycke, M. Conte, P. Bruzzi, and J. Michon. 2008. "Treatment of localised resectable neuroblastoma. Results of the LNESG1 study by the SIOP Europe Neuroblastoma Group." *Br J Cancer* 99 (7):1027-33.

Degoutin, J., N. Brunet-de Carvalho, C. Cifuentes-Diaz, and M. Vigny. 2009. "ALK (Anaplastic Lymphoma Kinase) expression in DRG neurons and its involvement in neuron-Schwann cells interaction." *Eur J Neurosci* 29 (2):275-86.

Diez del Corral, R., I. Olivera-Martinez, A. Goriely, E. Gale, M. Maden, and K. Storey. 2003. "Opposing FGF and retinoid pathways control ventral neural pattern, neuronal differentiation, and segmentation during body axis extension." *Neuron* 40 (1):65-79.

Duester, G. 2008. "Retinoic acid synthesis and signaling during early organogenesis." *Cell* 134 (6):921-31.

Ehlers, M. D. 2007. "Secrets of the secretory pathway in dendrite growth." *Neuron* 55 (5):686-9.

Espenshade, P., R. E. Gimeno, E. Holzmacher, P. Teung, and C. A. Kaiser. 1995. "Yeast SEC16 gene encodes a multidomain vesicle coat protein that interacts with Sec23p." *J Cell Biol* 131 (2):311-24.

Etienne-Manneville, S., and A. Hall. 2003. "Cdc42 regulates GSK-3beta and adenomatous polyposis coli to control cell polarity." *Nature* 421 (6924):753-6.

Evans, G. J., and M. A. Cousin. 2005. "Tyrosine phosphorylation of synaptophysin in synaptic vesicle recycling." *Biochem Soc Trans* 33 (Pt 6):1350-3.

Feng, S., C. Kasahara, R. J. Rickles, and S. L. Schreiber. 1995. "Specific interactions outside the proline-rich core of two classes of Src homology 3 ligands." *Proc Natl Acad Sci U S A* 92 (26):12408-15.

Foletti, D. L., R. Prekeris, and R. H. Scheller. 1999. "Generation and maintenance of neuronal polarity: mechanisms of transport and targeting." *Neuron* 23 (4):641-4.

Gardiol, A., C. Racca, and A. Triller. 1999. "Dendritic and postsynaptic protein synthetic machinery." *J Neurosci* 19 (1):168-79.

Gauthier, N. C., O. M. Rossier, A. Mathur, J. C. Hone, and M. P. Sheetz. 2009. "Plasma membrane area increases with spread area by exocytosis of a GPI-anchored protein compartment." *Mol Biol Cell* 20 (14):3261-72.

George, R. E., T. Sanda, M. Hanna, S. Frohling, W. Luther, 2nd, J. Zhang, Y. Ahn, W. Zhou, W. B. London, P. McGrady, L. Xue, S. Zozulya, V. E. Gregor, T. R. Webb, N. S. Gray, D. G. Gilliland, L. Diller, H. Greulich, S. W. Morris, M. Meyerson, and A. T. Look. 2008. "Activating mutations in ALK provide a therapeutic target in neuroblastoma." *Nature* 455 (7215):975-8.

Gherardi, S., E. Valli, D. Erriquez, and G. Perini. 2013. "MYCN-mediated transcriptional repression in neuroblastoma: the other side of the coin." *Front Oncol* 3:42.

Giraudo, C. G., and H. J. Maccioni. 2003. "Endoplasmic reticulum export of glycosyltransferases depends on interaction of a cytoplasmic dibasic motif with Sar1." *Mol Biol Cell* 14 (9):3753-66.

Glover, J. C., J. S. Renaud, and F. M. Rijli. 2006. "Retinoic acid and hindbrain patterning." *J Neurobiol* 66 (7):705-25.

Godden, T. M., R. Suman, M. J. Humphry, J. M. Rodenburg, and A. M. Maiden. 2014. "Principles and applications of a ptychographic microscope for three-dimensional imaging." *Microscopy and Analysis* 28(6):S10 – S13.

Goldsby, R. E., and K. K. Matthay. 2004. "Neuroblastoma: evolving therapies for a disease with many faces." *Paediatr Drugs* 6 (2):107-22.

Gordon, D. E., L. M. Bond, D. A. Sahlender, and A. A. Peden. 2010. "A targeted siRNA screen to identify SNAREs required for constitutive secretion in mammalian cells." *Traffic* 11 (9):1191-204.

Gumbiner, B. M. 1996. "Cell adhesion: the molecular basis of tissue architecture and morphogenesis." *Cell* 84 (3):345-57.

Hanafusa, H. 1987. "Functional and Structural Analysis of the v-src and c-src Genes." *Schettler G. (eds) Molecular Biology of the Arterial Wall.* vol 1987/88 / 1987/4.

Hedborg, F., C. Bjelfman, P. Sparen, B. Sandstedt, and S. Pahlman. 1995. "Biochemical evidence for a mature phenotype in morphologically poorly differentiated neuroblastomas with a favourable outcome." *Eur J Cancer* 31a (4):435-43.

Hernández Pérez, I. 2015. "The role of the COPII complex in neuroblastoma differentiation by N2-Src." MSc by Research thesis.

Hilfiker, S., V. A. Pieribone, A. J. Czernik, H. T. Kao, G. J. Augustine, and P. Greengard. 1999. "Synapsins as regulators of neurotransmitter release." *Philos Trans R Soc Lond B Biol Sci* 354 (1381):269-79.

Hoffmann, F. M., L. D. Fresco, H. Hoffman-Falk, and B. Z. Shilo. 1983. "Nucleotide sequences of the Drosophila src and abl homologs: conservation and variability in the src family oncogenes." *Cell* 35 (2 Pt 1):393-401.

Horton, A. C., and M. D. Ehlers. 2003. "Neuronal polarity and trafficking." *Neuron* 40 (2):277-95.

Horton, A. C., and M. D. Ehlers. 2004. "Secretory trafficking in neuronal dendrites." *Nat Cell Biol* 6 (7):585-91.

Horton, A. C., B. Racz, E. E. Monson, A. L. Lin, R. J. Weinberg, and M. D. Ehlers. 2005. "Polarized secretory trafficking directs cargo for asymmetric dendrite growth and morphogenesis." *Neuron* 48 (5):757-71.

Hsia, D. A., S. K. Mitra, C. R. Hauck, D. N. Streblow, J. A. Nelson, D. Ilic, S. Huang, E. Li, G. R. Nemerow, J. Leng, K. S. Spencer, D. A. Cheresh, and D. D. Schlaepfer. 2003. "Differential regulation of cell motility and invasion by FAK." *J Cell Biol* 160 (5):753-67.

Huber, K. 2006. "The sympathoadrenal cell lineage: specification, diversification, and new perspectives." *Dev Biol* 298 (2):335-43.

Hurley, S. P., D. O. Clary, V. Copie, and F. Lefcort. 2006. "Anaplastic lymphoma kinase is dynamically expressed on subsets of motor neurons and in the peripheral nervous system." *J Comp Neurol* 495 (2):202-12.

Huttenlocher, A. 2005. "Cell polarization mechanisms during directed cell migration." *Nat Cell Biol* 7 (4):336-7.

Huyer, G., S. Liu, J. Kelly, J. Moffat, P. Payette, B. Kennedy, G. Tsaprailis, M. J. Gresser, and C. Ramachandran. 1997. "Mechanism of inhibition of protein-tyrosine phosphatases by vanadate and pervanadate." *J Biol Chem* 272 (2):843-51.

Ikeda, H., B. Lethe, F. Lehmann, N. van Baren, J. F. Baurain, C. de Smet, H. Chambost, M. Vitale, A. Moretta, T. Boon, and P. G. Coulie. 1997. "Characterization of an antigen that is recognized on a melanoma showing partial HLA loss by CTL expressing an NK inhibitory receptor." *Immunity* 6 (2):199-208.

Ishida, T., M. Ishida, J. Suero, M. Takahashi, and B. C. Berk. 1999. "Agonist-stimulated cytoskeletal reorganization and signal transduction at focal adhesions in vascular smooth muscle cells require c-Src." *J Clin Invest* 103 (6):789-97.

Ishizawar, R., and S. J. Parsons. 2004. "c-Src and cooperating partners in human cancer." *Cancer Cell* 6 (3):209-14.

Iwahara, T., J. Fujimoto, D. Wen, R. Cupples, N. Bucay, T. Arakawa, S. Mori, B. Ratzkin, and T. Yamamoto. 1997. "Molecular characterization of ALK, a receptor tyrosine kinase expressed specifically in the nervous system." *Oncogene* 14 (4):439-49.

Iyer, S. C., E. P. Ramachandran Iyer, R. Meduri, M. Rubaharan, A. Kuntimaddi, M. Karamsetty, and D. N. Cox. 2013. "Cut, via CrebA, transcriptionally regulates the COPII secretory pathway to direct dendrite development in Drosophila." *J Cell Sci* 126 (Pt 20):4732-45.

Jain, P., R. A. Worthylake, and S. K. Alahari. 2012. "Quantitative analysis of random migration of cells using time-lapse video microscopy." *J Vis Exp* (63):e3585.

Janoueix-Lerosey, I., D. Lequin, L. Brugieres, A. Ribeiro, L. de Pontual, V. Combaret, V. Raynal, A. Puisieux, G. Schleiermacher, G. Pierron, D. Valteau-Couanet, T. Frebourg, J. Michon, S. Lyonnet, J. Amiel, and O. Delattre. 2008. "Somatic and germline activating mutations of the ALK kinase receptor in neuroblastoma." *Nature* 455 (7215):967-70.

Jonkman, J. E., J. A. Cathcart, F. Xu, M. E. Bartolini, J. E. Amon, K. M. Stevens, and P. Colarusso. 2014. "An introduction to the wound healing assay using live-cell microscopy." *Cell Adh Migr* 8 (5):440-51.

Kalia, L. V., J. R. Gingrich, and M. W. Salter. 2004. "Src in synaptic transmission and plasticity." *Oncogene* 23 (48):8007-16.

Kang, C. B., Y. Hong, S. Dhe-Paganon, and H. S. Yoon. 2008. "FKBP family proteins: immunophilins with versatile biological functions." *Neurosignals* 16 (4):318-25.

Keenan, S., P. A. Lewis, S. J. Wetherill, C. J. Dunning, and G. J. Evans. 2015. "The N2-Src neuronal splice variant of C-Src has altered SH3 domain ligand specificity and a higher constitutive activity than N1-Src." *FEBS Lett* 589 (15):1995-2000.

Keenan, S., S. J. Wetherill, C. I. Ugbode, S. Chawla, W. J. Brackenbury, and G. J. Evans. 2017. "Inhibition of N1-Src kinase by a specific SH3 peptide ligand reveals a role for N1-Src in neurite elongation by L1-CAM." *Sci Rep* 7:43106.

Kelley, M. W., J. K. Turner, and T. A. Reh. 1994. "Retinoic acid promotes differentiation of photoreceptors in vitro." *Development* 120 (8):2091-102.

Kleiner-Bossaler, A., and H. F. Deluca. 1971. "Formation of retinoic acid from retinol in the kidney." *Arch Biochem Biophys* 142 (1):371-7.

Korpal, M., B. J. Ell, F. M. Buffa, T. Ibrahim, M. A. Blanco, T. Celia-Terrassa, L. Mercatali, Z. Khan, H. Goodarzi, Y. Hua, Y. Wei, G. Hu, B. A. Garcia, J. Ragoussis, D. Amadori, A. L. Harris, and Y. Kang. 2011. "Direct targeting of Sec23a by miR-200s influences cancer cell secretome and promotes metastatic colonization." *Nat Med* 17 (9):1101-8.

Kupfer, A., G. Dennert, and S. J. Singer. 1983. "Polarization of the Golgi apparatus and the microtubule-organizing center within cloned natural killer cells bound to their targets." *Proc Natl Acad Sci U S A* 80 (23):7224-8.

Lang, M. R., L. A. Lapierre, M. Frotscher, J. R. Goldenring, and E. W. Knapik. 2006. "Secretory COPII coat component Sec23a is essential for craniofacial chondrocyte maturation." *Nat Genet* 38 (10):1198-203.

Larsen, WJ. 2001. "Human Embryology." Third ed.

Le Lièvre, C. S., and N. M. Le Douarin. 1975. "Mesenchymal derivatives of the neural crest: analysis of chimaeric quail and chick embryos." *J Embryol Exp Morphol* 34 (1):125-54.

Lecuit, T., and F. Pilot. 2003. "Developmental control of cell morphogenesis: a focus on membrane growth." *Nat Cell Biol* 5 (2):103-8.

Lewis, P. 2014. "The role of N-Src kinases in neuronal differentiation." PhD thesis.

Liang, C. C., A. Y. Park, and J. L. Guan. 2007. "In vitro scratch assay: a convenient and inexpensive method for analysis of cell migration in vitro." *Nat Protoc* 2 (2):329-33.

Maiden, A. M., and J. M. Rodenburg. 2009. "An improved ptychographical phase retrieval algorithm for diffractive imaging." *Ultramicroscopy* 109 (10):1256-62.

Maris, J. M. 2010. "Recent advances in neuroblastoma." *N Engl J Med* 362 (23):2202-11.

Maris, J. M., M. D. Hogarty, R. Bagatell, and S. L. Cohn. 2007. "Neuroblastoma." *Lancet* 369 (9579):2106-20.

Marrison, J., L. Raty, P. Marriott, and P. O'Toole. 2013. "Ptychography--a label free, high-contrast imaging technique for live cells using quantitative phase information." *Sci Rep* 3:2369.

Marshall, G. M., D. R. Carter, B. B. Cheung, T. Liu, M. K. Mateos, J. G. Meyerowitz, and W. A. Weiss. 2014. "The prenatal origins of cancer." *Nat Rev Cancer* 14 (4):277-89.

Martin, G. S. 2001. "The hunting of the Src." *Nat Rev Mol Cell Biol* 2 (6):467-75.

Martin, G. S. 2004. "The road to Src." *Oncogene* 23 (48):7910-7.

Mathsyaraja, H., and R. N. Eisenman. 2016. "Parsing Myc Paralogs in Oncogenesis." *Cancer Cell* 29 (1):1-2.

Matsunaga, T., H. Shirasawa, H. Enomoto, H. Yoshida, J. Iwai, M. Tanabe, K. Kawamura, T. Etoh, and N. Ohnuma. 1998. "Neuronal src and trk a protooncogene expression in neuroblastomas and patient prognosis." *Int J Cancer* 79 (3):226-31.

Matsunaga, T., H. Shirasawa, M. Tanabe, N. Ohnuma, H. Takahashi, and B. Simizu. 1993. "Expression of alternatively spliced src messenger RNAs related to neuronal differentiation in human neuroblastomas." *Cancer Res* 53 (13):3179-85.

Matthay, K. K., C. P. Reynolds, R. C. Seeger, H. Shimada, E. S. Adkins, D. Haas-Kogan, R. B. Gerbing, W. B. London, and J. G. Villablanca. 2009. "Long-term results for children with high-risk neuroblastoma treated on a randomized trial of myeloablative therapy followed by 13-cis-retinoic acid: a children's oncology group study." *J Clin Oncol* 27 (7):1007-13.

Matthay, K. K., J. G. Villablanca, R. C. Seeger, D. O. Stram, R. E. Harris, N. K. Ramsay, P. Swift, H. Shimada, C. T. Black, G. M. Brodeur, R. B. Gerbing, and C. P. Reynolds. 1999. "Treatment of high-risk neuroblastoma with intensive chemotherapy, radiotherapy, autologous bone marrow transplantation, and 13-cis-retinoic acid. Children's Cancer Group." *N Engl J Med* 341 (16):1165-73.

Matthay, Katherine K., John M. Maris, Gudrun Schleiermacher, Akira Nakagawara, Crystal L. Mackall, Lisa Diller, and William A. Weiss. 2016. "Neuroblastoma." 2:16078.

Mayer, Erica L., and Ian E. Krop. 2010. "Advances in Targeting Src in the Treatment of Breast Cancer and Other Solid Malignancies."

McPherson, P. S., A. J. Czernik, T. J. Chilcote, F. Onofri, F. Benfenati, P. Greengard, J. Schlessinger, and P. De Camilli. 1994. "Interaction of Grb2 via its Src homology 3 domains with synaptic proteins including synapsin I." *Proc Natl Acad Sci U S A* 91 (14):6486-90.

Mellstrom, K., C. Bjelfman, U. Hammerling, and S. Pahlman. 1987. "Expression of c-src in cultured human neuroblastoma and small-cell lung carcinoma cell lines correlates with neurocrine differentiation." *Mol Cell Biol* 7 (12):4178-84.

Mertens, A. C., Y. Yasui, J. P. Neglia, J. D. Potter, M. E. Nesbit, Jr., K. Ruccione, W. A. Smithson, and L. L. Robison. 2001. "Late mortality experience in five-year survivors of childhood and adolescent cancer: the Childhood Cancer Survivor Study." *J Clin Oncol* 19 (13):3163-72.

Miller, E. A., T. H. Beilharz, P. N. Malkus, M. C. Lee, S. Hamamoto, L. Orci, and R. Schekman. 2003. "Multiple cargo binding sites on the COPII subunit Sec24p ensure capture of diverse membrane proteins into transport vesicles." *Cell* 114 (4):497-509.

Miller, E., B. Antonny, S. Hamamoto, and R. Schekman. 2002. "Cargo selection into COPII vesicles is driven by the Sec24p subunit." *Embo j* 21 (22):6105-13.

Moroco, J. A., J. K. Craigo, R. E. Iacob, T. E. Wales, J. R. Engen, and T. E. Smithgall. 2014. "Differential sensitivity of Src-family kinases to activation by SH3 domain displacement." *PLoS One* 9 (8):e105629.

Morris, S. W., C. Naeve, P. Mathew, P. L. James, M. N. Kirstein, X. Cui, and D. P. Witte. 1997. "ALK, the chromosome 2 gene locus altered by the t(2;5) in non-Hodgkin's lymphoma, encodes a novel neural receptor tyrosine kinase that is highly related to leukocyte tyrosine kinase (LTK)." *Oncogene* 14 (18):2175-88.

Mosse, Y. P., M. Laudenslager, L. Longo, K. A. Cole, A. Wood, E. F. Attiyeh, M. J. Laquaglia, R. Sennett, J. E. Lynch, P. Perri, G. Laureys, F. Speleman, C. Kim, C. Hou, H. Hakonarson, A. Torkamani, N. J. Schork, G. M. Brodeur, G. P. Tonini, E. Rappaport, M. Devoto, and J. M. Maris. 2008. "Identification of ALK as a major familial neuroblastoma predisposition gene." *Nature* 455 (7215):930-5.

Mosse, Y. P., A. Wood, and J. M. Maris. 2009. "Inhibition of ALK signaling for cancer therapy." *Clin Cancer Res* 15 (18):5609-14.

Mossessova, E., L. C. Bickford, and J. Goldberg. 2003. "SNARE selectivity of the COPII coat." *Cell* 114 (4):483-95.

Mullany, P. M., and M. A. Lynch. 1998. "Evidence for a role for synaptophysin in expression of long-term potentiation in rat dentate gyrus." *Neuroreport* 9 (11):2489-94.

Nakano, A., and M. Muramatsu. 1989. "A novel GTP-binding protein, Sar1p, is involved in transport from the endoplasmic reticulum to the Golgi apparatus." *J Cell Biol* 109 (6 Pt 1):2677-91.

Niederreither, K., and P. Dolle. 2008. "Retinoic acid in development: towards an integrated view." *Nat Rev Genet* 9 (7):541-53.

Nikolopoulou, E., G. L. Galea, A. Rolo, N. D. Greene, and A. J. Copp. 2017. "Neural tube closure: cellular, molecular and biomechanical mechanisms." *Development* 144 (4):552-566.

Nuchtern, J. G., W. B. London, C. E. Barnewolt, A. Naranjo, P. W. McGrady, J. D. Geiger, L. Diller, M. L. Schmidt, J. M. Maris, S. L. Cohn, and R. C. Shamberger. 2012. "A prospective study of expectant observation as primary therapy for neuroblastoma in young infants: a Children's Oncology Group study." *Ann Surg* 256 (4):573-80.

O'Toole, P., and R. Suman. 2014. "Label-free cell imaging." *G.I.T. Imaging and Microscopy* 16(3) 26.

Oberthuer, A., B. Hero, R. Spitz, F. Berthold, and M. Fischer. 2004. "The tumor-associated antigen PRAME is universally expressed in high-stage neuroblastoma and associated with poor outcome." *Clin Cancer Res* 10 (13):4307-13.

Onofri, F., S. Giovedi, H. T. Kao, F. Valtorta, L. Bongiorno Borbone, P. De Camilli, P. Greengard, and F. Benfenati. 2000. "Specificity of the binding of synapsin I to Src homology 3 domains." *J Biol Chem* 275 (38):29857-67.

Onofri, F., S. Giovedi, P. Vaccaro, A. J. Czernik, F. Valtorta, P. De Camilli, P. Greengard, and F. Benfenati. 1997. "Synapsin I interacts with c-Src and stimulates its tyrosine kinase activity." *Proc Natl Acad Sci U S A* 94 (22):12168-73.

Onofri, F., M. Messa, V. Matafora, G. Bonanno, A. Corradi, A. Bachi, F. Valtorta, and F. Benfenati. 2007. "Synapsin phosphorylation by SRC tyrosine kinase enhances SRC activity in synaptic vesicles." *J Biol Chem* 282 (21):15754-67.

Oppermann, H., A. D. Levinson, H. E. Varmus, L. Levintow, and J. M. Bishop. 1979. "Uninfected vertebrate cells contain a protein that is closely related to the product of the avian sarcoma virus transforming gene (src)." *Proc Natl Acad Sci U S A* 76 (4):1804-8.

Palmer, R. H., E. Vernersson, C. Grabbe, and B. Hallberg. 2009. "Anaplastic lymphoma kinase: signalling in development and disease." *Biochem J* 420 (3):345-61.

Parker, R. C., G. Mardon, R. V. Lebo, H. E. Varmus, and J. M. Bishop. 1985. "Isolation of duplicated human c-src genes located on chromosomes 1 and 20." *Mol Cell Biol* 5 (4):831-8.

Parker, R. C., H. E. Varmus, and J. M. Bishop. 1981. "Cellular homologue (c-src) of the transforming gene of Rous sarcoma virus: isolation, mapping, and transcriptional analysis of c-src and flanking regions." *Proc Natl Acad Sci U S A* 78 (9):5842-6.

Parsons, S. J., and J. T. Parsons. 2004. "Src family kinases, key regulators of signal transduction." *Oncogene* 23 (48):7906-9.

Paul, G., J. Cardinale, and I. F. Sbalzarini. 2013. "Coupling Image Restoration and Segmentation: A Generalized Linear Model/Bregman Perspective." *Int J Comput Vis*.

PDQ, Pediatric Treatment Editorial Board. 2017. "Neuroblastoma Treatment (PDQ®): Health Professional Version." *PDQ Cancer Information Summaries. Bethesda (MD): National Cancer Institute (US).*

Petrie, R. J., A. D. Doyle, and K. M. Yamada. 2009. "Random versus directionally persistent cell migration." *Nat Rev Mol Cell Biol* 10 (8):538-49.

Pierce, J. P., T. Mayer, and J. B. McCarthy. 2001. "Evidence for a satellite secretory pathway in neuronal dendritic spines." *Curr Biol* 11 (5):351-5.

Pinto, N. R., M. A. Applebaum, S. L. Volchenboum, K. K. Matthay, W. B. London, P. F. Ambros, A. Nakagawara, F. Berthold, G. Schleiermacher, J. R. Park, D. Valteau-Couanet, A. D. Pearson, and S. L. Cohn. 2015. "Advances in Risk Classification and Treatment Strategies for Neuroblastoma." *J Clin Oncol* 33 (27):3008-17.

Poujade, M., E. Grasland-Mongrain, A. Hertzog, J. Jouanneau, P. Chavrier, B. Ladoux, A. Buguin, and P. Silberzan. 2007. "Collective migration of an epithelial monolayer in response to a model wound." *Proc Natl Acad Sci U S A* 104 (41):15988-93.

Prager-Khoutorsky, M., and M. E. Spira. 2009. "Neurite retraction and regrowth regulated by membrane retrieval, membrane supply, and actin dynamics." *Brain Res* 1251:65-79.

Pyper, J. M., and J. B. Bolen. 1989. "Neuron-specific splicing of C-SRC RNA in human brain." *J Neurosci Res* 24 (1):89-96.

Qiao, J., S. Lee, P. Paul, L. Qiao, C. J. Taylor, C. Schlegel, N. C. Colon, and D. H. Chung. 2013. "Akt2 regulates metastatic potential in neuroblastoma." *PLoS One* 8 (2):e56382.

Raulf, F., S. M. Robertson, and M. Schartl. 1989. "Evolution of the neuron-specific alternative splicing product of the c-src proto-oncogene." *J Neurosci Res* 24 (1):81-8.

Reissmann, E., U. Ernsberger, P. H. Francis-West, D. Rueger, P. M. Brickell, and H. Rohrer. 1996. "Involvement of bone morphogenetic protein-4 and bone morphogenetic protein-7 in the

differentiation of the adrenergic phenotype in developing sympathetic neurons." *Development* 122 (7):2079-88.

Reiterer, V., S. Maier, H. H. Sitte, A. Kriz, M. A. Ruegg, H. P. Hauri, M. Freissmuth, and H. Farhan. 2008. "Sec24- and ARFGAP1-dependent trafficking of GABA transporter-1 is a prerequisite for correct axonal targeting." *J Neurosci* 28 (47):12453-64.

Reynolds, C. P. 2004. "Detection and treatment of minimal residual disease in high-risk neuroblastoma." *Pediatr Transplant* 8 Suppl 5:56-66.

Rizk, A., G. Paul, P. Incardona, M. Bugarski, M. Mansouri, A. Niemann, U. Ziegler, P. Berger, and I. F. Sbalzarini. 2014. "Segmentation and quantification of subcellular structures in fluorescence microscopy images using Squassh." *Nat Protoc* 9 (3):586-96.

Rodriguez, L. G., X. Wu, and J. L. Guan. 2005. "Wound-healing assay." *Methods Mol Biol* 294:23-9.

Rollins, C. T., V. M. Rivera, D. N. Woolfson, T. Keenan, M. Hatada, S. E. Adams, L. J. Andrade, D. Yaeger, M. R. van Schravendijk, D. A. Holt, M. Gilman, and T. Clackson. 2000. "A ligand-reversible dimerization system for controlling protein-protein interactions." *Proc Natl Acad Sci U S A* 97 (13):7096-101.

Roskoski, R., Jr. 2015. "Src protein-tyrosine kinase structure, mechanism, and small molecule inhibitors." *Pharmacol Res* 94:9-25.

Rous, P. 1910a. "An Experimental Comparison of Transplanted Tumor and a Transplanted Normal Tissue Capable of Growth." *J Exp Med* 12 (3):344-66.

Rous, P. 1910b. "A Transmissible Avian Neoplasm. (Sarcoma of the Common Fowl.)." *J Exp Med* 12 (5):696-705.

Rubie, H., B. De Bernardi, M. Gerrard, A. Canete, R. Ladenstein, J. Couturier, P. Ambros, C. Munzer, A. D. Pearson, A. Garaventa, P. Brock, V. Castel, D. Valteau-Couanet, K. Holmes, A. Di Cataldo, B. Brichard, V. Mosseri, C. Marquez, D. Plantaz, L. Boni, and J. Michon. 2011. "Excellent outcome with reduced treatment in infants with nonmetastatic and unresectable neuroblastoma without MYCN amplification: results of the prospective INES 99.1." *J Clin Oncol* 29 (4):449-55.

Salama, N. R., T. Yeung, and R. W. Schekman. 1993. "The Sec13p complex and reconstitution of vesicle budding from the ER with purified cytosolic proteins." *Embo j* 12 (11):4073-82.

Schneider, C., H. Wicht, J. Enderich, M. Wegner, and H. Rohrer. 1999. "Bone morphogenetic proteins are required in vivo for the generation of sympathetic neurons." *Neuron* 24 (4):861-70.

Schwab, M., J. Ellison, M. Busch, W. Rosenau, H. E. Varmus, and J. M. Bishop. 1984. "Enhanced expression of the human gene N-myc consequent to amplification of DNA may contribute to malignant progression of neuroblastoma." *Proc Natl Acad Sci U S A* 81 (15):4940-4.

Shalloway, D., A. D. Zelenetz, and G. M. Cooper. 1981. "Molecular cloning and characterization of the chicken gene homologous to the transforming gene of Rous sarcoma virus." *Cell* 24 (2):531-41.

Short, Sarah M., Gregory A. Talbott, and Rudolph L. Juliano. 1998. "Integrin-mediated Signaling Events in Human Endothelial Cells."

Sicheri, F., and J. Kuriyan. 1997. "Structures of Src-family tyrosine kinases." *Curr Opin Struct Biol* 7 (6):777-85.

Sicheri, F., I. Moarefi, and J. Kuriyan. 1997. "Crystal structure of the Src family tyrosine kinase Hck." *Nature* 385 (6617):602-9.

Sieg, D. J., C. R. Hauck, D. Ilic, C. K. Klingbeil, E. Schaefer, C. H. Damsky, and D. D. Schlaepfer. 2000. "FAK integrates growth-factor and integrin signals to promote cell migration." *Nat Cell Biol* 2 (5):249-56.

Song, H. J., and M. M. Poo. 1999. "Signal transduction underlying growth cone guidance by diffusible factors." *Curr Opin Neurobiol* 9 (3):355-63.

Stafman, L. L., and E. A. Beierle. 2016. "Cell Proliferation in Neuroblastoma." *Cancers (Basel)* 8 (1).

Sternberg, S.R. 1983. "Biomedical Image Processing."

Sytnyk, V., I. Leshchyns'ka, M. Delling, G. Dityateva, A. Dityatev, and M. Schachner. 2002. "Neural cell adhesion molecule promotes accumulation of TGN organelles at sites of neuron-to-neuron contacts." *J Cell Biol* 159 (4):649-61.

Szczyrba, J., E. Nolte, S. Wach, E. Kremmer, R. Stohr, A. Hartmann, W. Wieland, B. Wullich, and F. A. Grasser. 2011. "Downregulation of Sec23A protein by miRNA-375 in prostate carcinoma." *Mol Cancer Res* 9 (6):791-800.

Takeya, T., R. A. Feldman, and H. Hanafusa. 1982. "DNA sequence of the viral and cellular src gene of chickens. 1. Complete nucleotide sequence of an EcoRI fragment of recovered avian sarcoma virus which codes for gp37 and pp60src." *J Virol* 44 (1):1-11.

Takeya, T., and H. Hanafusa. 1983. "Structure and sequence of the cellular gene homologous to the RSV src gene and the mechanism for generating the transforming virus." *Cell* 32 (3):881-890.

Tang, B. L. 2001. "Protein trafficking mechanisms associated with neurite outgrowth and polarized sorting in neurons." *J Neurochem* 79 (5):923-30.

Tang, B. L. 2008. "Emerging aspects of membrane traffic in neuronal dendrite growth." *Biochim Biophys Acta* 1783 (2):169-76.

Thomas, J. W., B. Ellis, R. J. Boerner, W. B. Knight, G. C. White, 2nd, and M. D. Schaller. 1998. "SH2- and SH3-mediated interactions between focal adhesion kinase and Src." *J Biol Chem* 273 (1):577-83.

Thomas, S. M., and J. S. Brugge. 1997. "Cellular functions regulated by Src family kinases." *Annu Rev Cell Dev Biol* 13:513-609.

Valent, P., D. Bonnet, R. De Maria, T. Lapidot, M. Copland, J. V. Melo, C. Chomienne, F. Ishikawa, J. J. Schuringa, G. Stassi, B. Huntly, H. Herrmann, J. Soulier, A. Roesch, G. J. Schuurhuis, S. Wohrer, M. Arock, J. Zuber, S. Cerny-Reiterer, H. E. Johnsen, M. Andreeff, and C. Eaves. 2012. "Cancer stem cell definitions and terminology: the devil is in the details." *Nat Rev Cancer* 12 (11):767-75.

Vernersson, E., N. K. Khoo, M. L. Henriksson, G. Roos, R. H. Palmer, and B. Hallberg. 2006. "Characterization of the expression of the ALK receptor tyrosine kinase in mice." *Gene Expr Patterns* 6 (5):448-61.

Wang, J., S. Davis, S. Menon, J. Zhang, J. Ding, S. Cervantes, E. Miller, Y. Jiang, and S. Ferro-Novick. 2015. "Ypt1/Rab1 regulates Hrr25/CK1δ kinase activity in ER–Golgi traffic and macroautophagy." In *J Cell Biol*, 273-85.

Watson, P., A. K. Townley, P. Koka, K. J. Palmer, and D. J. Stephens. 2006. "Sec16 defines endoplasmic reticulum exit sites and is required for secretory cargo export in mammalian cells." *Traffic* 7 (12):1678-87.

Wilde, B. R., and D. E. Ayer. 2015. "Interactions between Myc and MondoA transcription factors in metabolism and tumourigenesis." *Br J Cancer* 113 (11):1529-33.

Wilson, L. M., and G. J. Draper. 1974. "Neuroblastoma, its natural history and prognosis: a study of 487 cases." *Br Med J* 3 (5926):301-7.

Xu, W., A. Doshi, M. Lei, M. J. Eck, and S. C. Harrison. 1999. "Crystal structures of c-Src reveal features of its autoinhibitory mechanism." *Mol Cell* 3 (5):629-38.

Yang, X. M., R. Martinez, J. Le Beau, O. Wiestler, and G. Walter. 1989. "Evolutionary expression of the neuronal form of the src protein in the brain." *Proc Natl Acad Sci U S A* 86 (12):4751-5.

Ye, B., Y. Zhang, W. Song, S. H. Younger, L. Y. Jan, and Y. N. Jan. 2007. "Growing dendrites and axons differ in their reliance on the secretory pathway." *Cell* 130 (4):717-29.

Yuan, J., and B. A. Yankner. 2000. "Apoptosis in the nervous system." *Nature* 407 (6805):802-9.

Zhao, W., S. Cavallaro, P. Gusev, and D. L. Alkon. 2000. "Nonreceptor tyrosine protein kinase pp60c-src in spatial learning: synapse-specific changes in its gene expression, tyrosine phosphorylation, and protein-protein interactions." *Proc Natl Acad Sci U S A* 97 (14):8098-103.

Zhu, M., J. Tao, M. P. Vasievich, W. Wei, G. Zhu, R. N. Khoriaty, and B. Zhang. 2015. "Neural tube opening and abnormal extraembryonic membrane development in SEC23A deficient mice." *Sci Rep* 5:15471.

Zimmerman, K. A., G. D. Yancopoulos, R. G. Collum, R. K. Smith, N. E. Kohl, K. A. Denis, M. M. Nau, O. N. Witte, D. Toran-Allerand, C. E. Gee, and et al. 1986. "Differential expression of myc family genes during murine development." *Nature* 319 (6056):780-3.